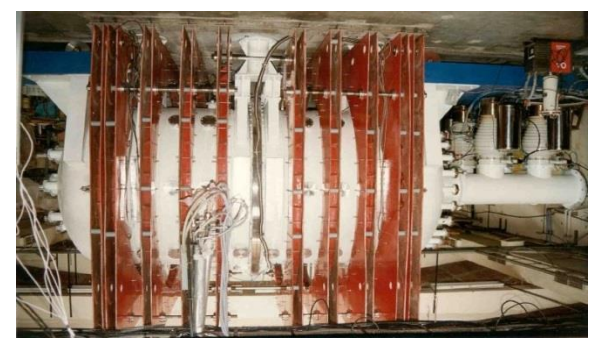




Institute for Plasma Research,
Gandhinagar, India



Large Volume Plasma Device

Experimental Study on ETG Turbulence Induced Plasma Transport in Large Volume Plasma Device

Prabhakar Srivastav

*e-mail: prabhakar.srivastav@ipr.res.in

$$\Omega_{ci} < \omega \ll \Omega_{ce}$$

$$k_{\perp} \rho_e \leq 1$$

Talk at PPPL (August 28, 2019)

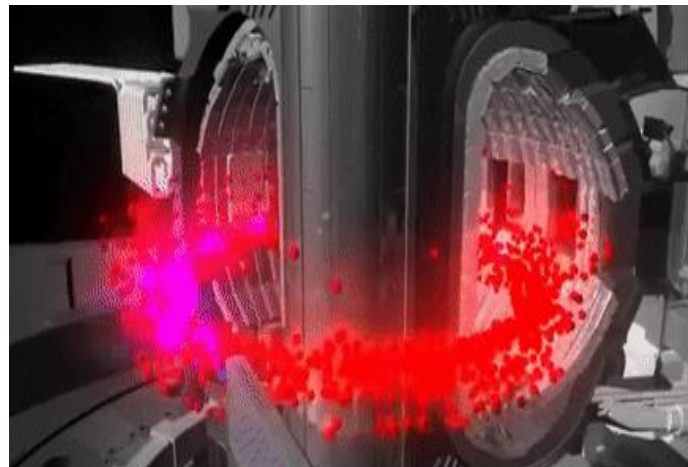
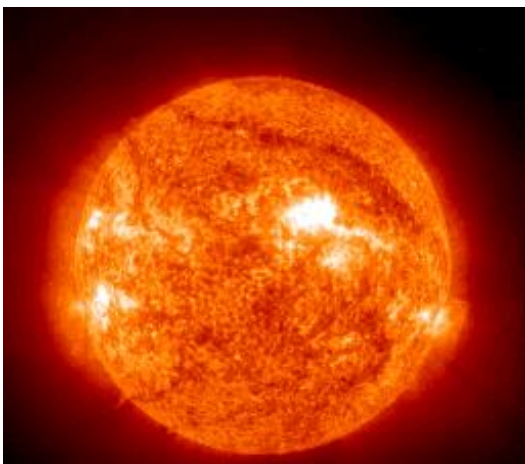


Outline

- **Introduction**
- **Experimental setup**
- **Identification of ETG instability in LVPD**
- **Investigation of particle and energy transport,**
 - **Electrostatic particle flux** ($\Gamma_{es} = \langle \delta n_e \delta v_r \rangle$)
 - **Electromagnetic particle flux** ($\Gamma_{em} = \frac{\langle \delta J_{\parallel, q} \delta B_r \rangle}{qB}$)
 - **Total heat flux** ($Q_{total} = \frac{3}{2} \langle \delta p_e \delta v_r \rangle$)
- **Summary & conclusion**



Introduction



- ❖ Transport involves study of physical processes responsible for particles, momentum and energy displacement.
- ❖ Transport determines the profile of the system self-consistently.
- ❖ Transport in plasma can be understood under the following three categories namely,
 1. **Classical transport** $\propto \nu (\lambda_f^2)$
 2. **Neo-classical transport** $\propto \nu (\lambda_f^2)(1+2q^2)$ [in tokamaks]
 3. **Turbulent transport** $\propto |\tilde{\phi}|^2$



Introduction

- ❖ **Turbulent Transport is a universal phenomenon present in laboratory, space and astrophysical systems.**
- ❖ **Turbulence leads to generation of particle as well as heat transport of the order of magnitudes higher than the classical and neoclassical flux predictions in fusion devices.**
- ❖ **This anomalous flux is attributed to turbulent fluctuations due to various instabilities inherent in the system.**
- ❖ **Confined systems are naturally inhomogeneous which act as source of free energy to drive the system, any perturbations can evolve over a wide range of scale, from electron to ion and up to system scale.**
- ❖ **Large scale perturbations are easy to probe in tokamaks and tremendous progress has already been made on ion temperature gradient driven micro-turbulent mode ($k_{\perp}\rho_i \leq 1$) and MHD modes.**



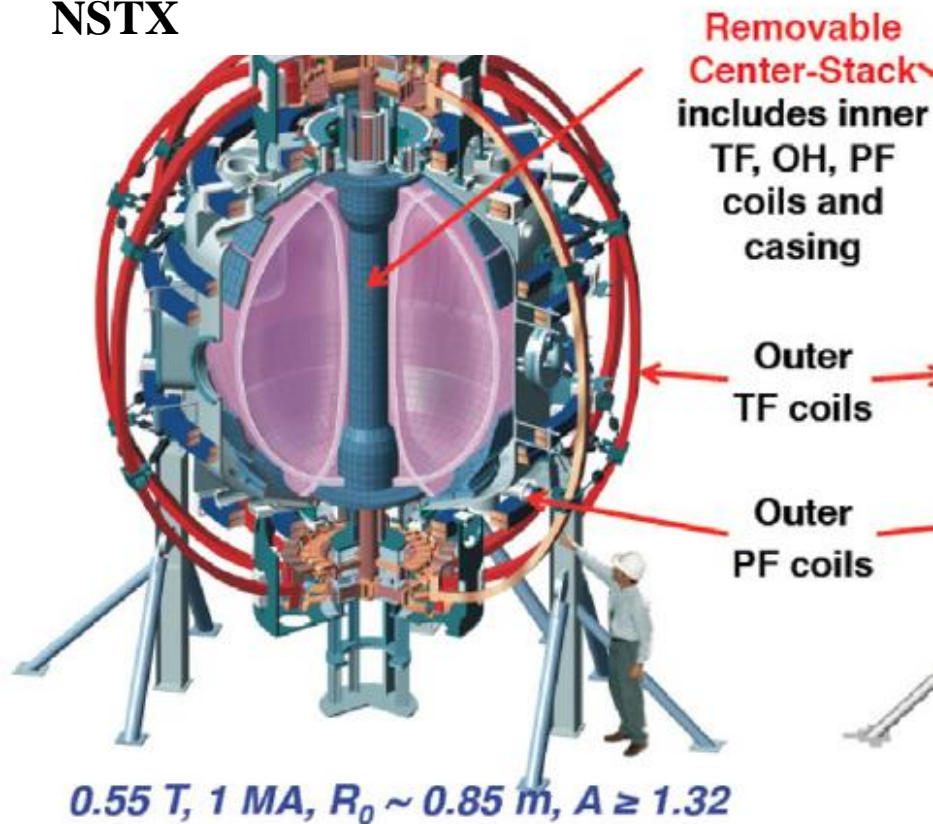
Introduction

- Small scale fluctuations, of the order of electron scale excited due to electron temperature gradient in high magnetic field (\sim Tesla) of tokamak are difficult to probe ($k_{\perp}\rho_e \leq 1$).

Tore Supra (WEST)



NSTX

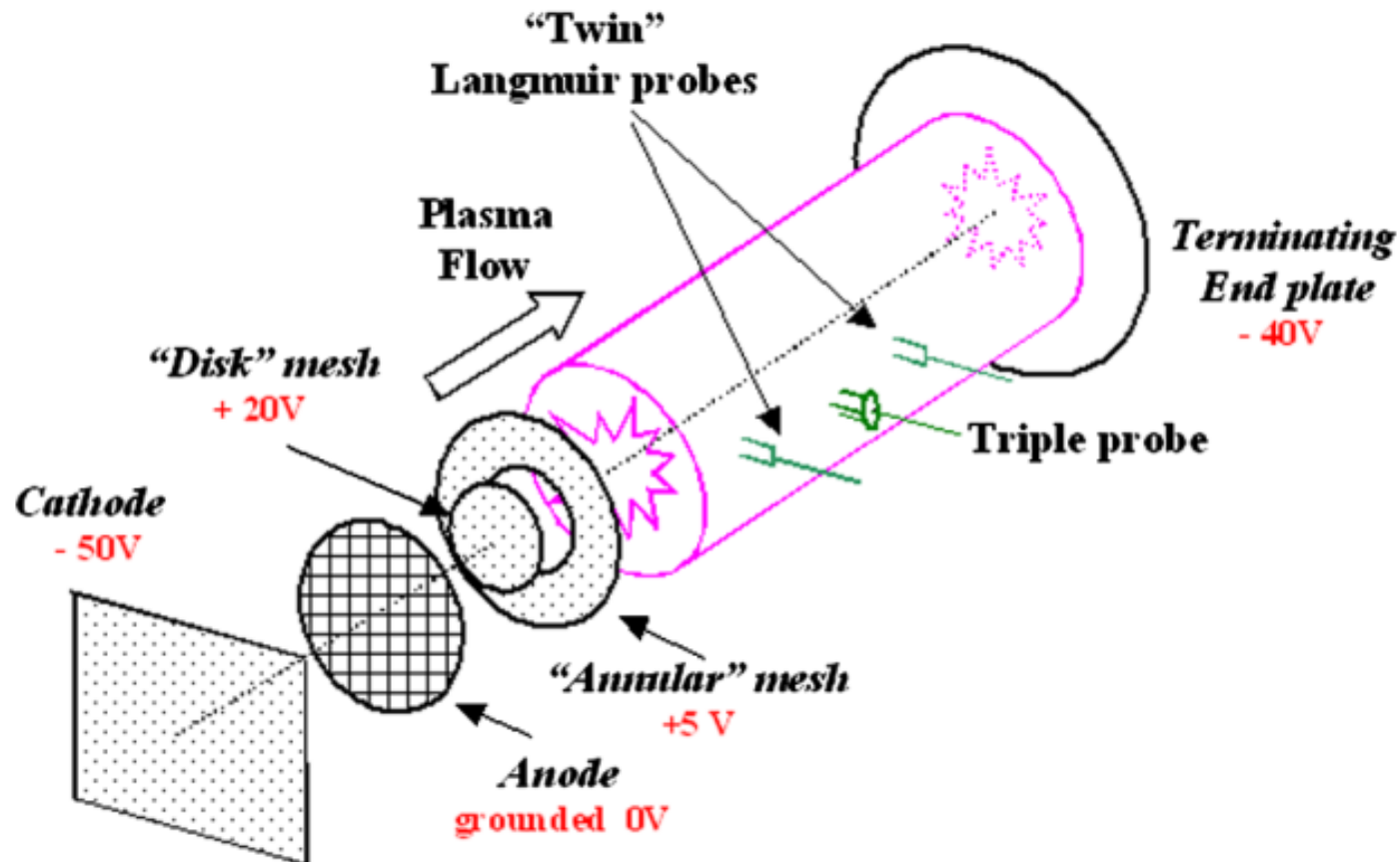


- ❖ Tore Supra, (Horton *et al.* Phys. Plasmas, Vol. 11, No. 5, (2004))
- ❖ NSTX, (Mazzucato *et al.* Phys. Rev. Lett. 101, 075001 (2008))



Introduction

- ❖ To understand such small scales fluctuation some linear devices like Columbia Linear Machine (CLM), Large Volume Plasma Device (LVPD) have taken initiatives.



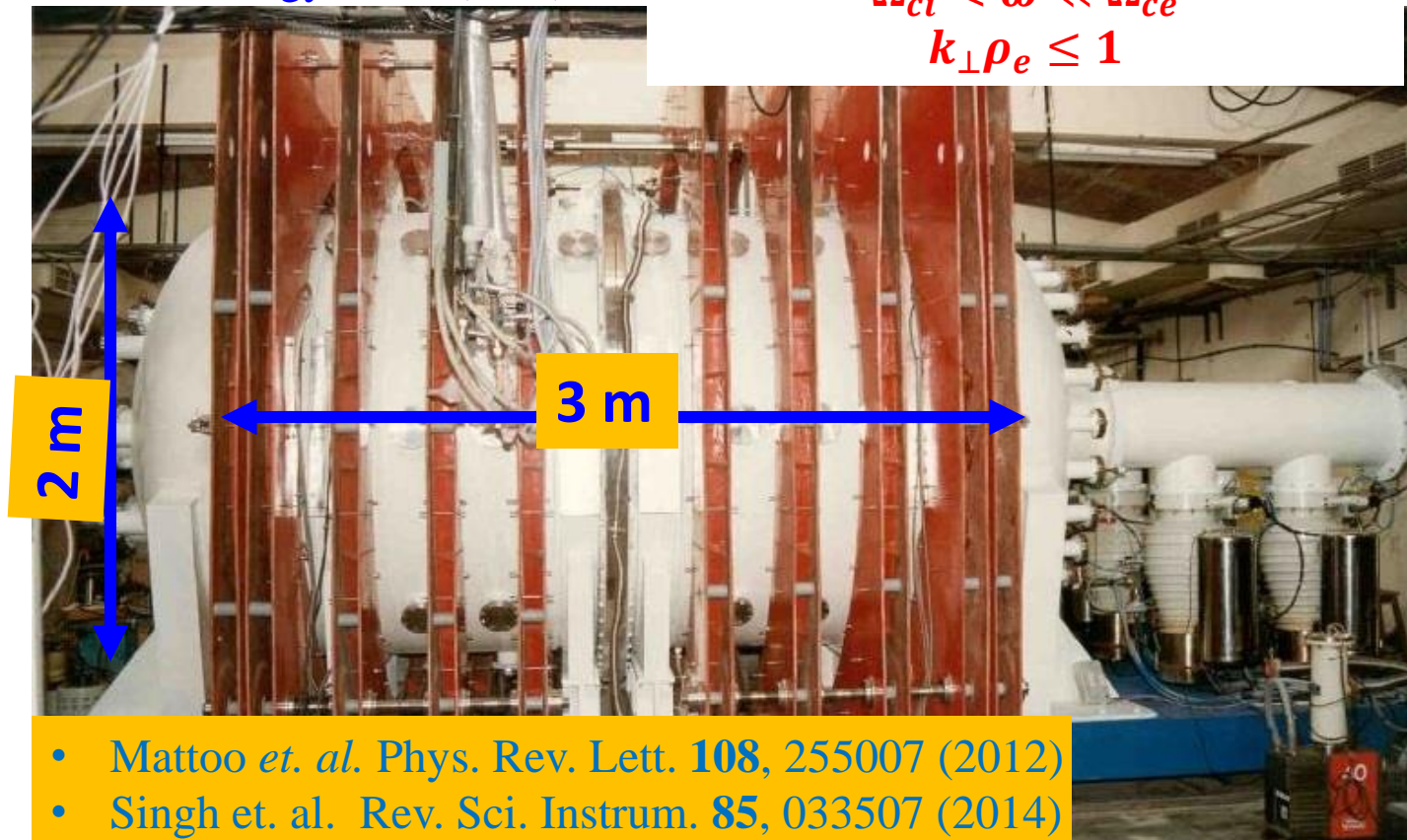
- ❖ X. Wei *et. al.* Phys. Plasmas **17**, 042108 (2010)
- ❖ V. Sokolov and A. K. Sen, Phys. Rev. Lett. **107**, 155001 (2011)
- ❖ Fu *et al.* Phys. Plasmas **19**, 032303 (2012)



Introduction

- ❖ In LVPD with finite plasma beta, $\beta \sim (0.06 - 0.4)$, electron temperature gradient driven turbulence is observed in energetic electrons free plasma by making use of large Electron Energy Filter (EEF) .

$$\Omega_{ci} < \omega \ll \Omega_{ce}$$
$$k_{\perp} \rho_e \leq 1$$



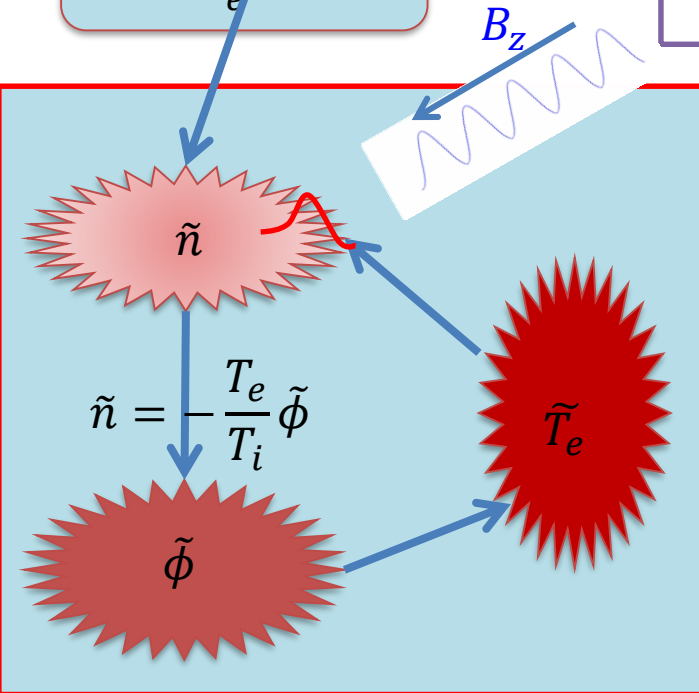
- **What is the role of ETG scale fluctuation on plasma transport in LVPD?**



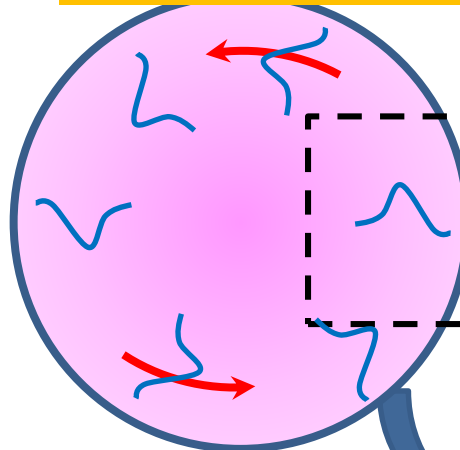
Turbulent Transport Mechanism

$$\Gamma = \langle \tilde{n}_e \tilde{v}_r \rangle = - \sum_k \frac{k_y}{B} |\tilde{n}_{e,k}| |\tilde{\Phi}_k| \gamma_{n\phi} \sin \theta_{n_e \phi}$$

Free Energy
 ∇T_e

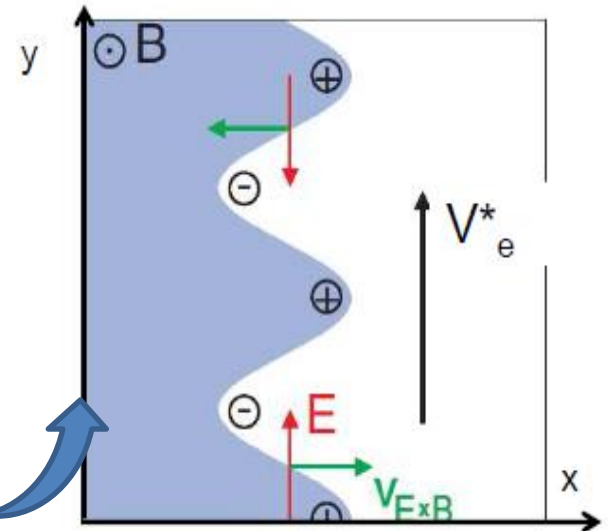


$$V_{D,q} = - \frac{\nabla p \times B_z}{qnB_z^2}$$



$$J_\theta \times B_z = \nabla p$$

1. Particle Flux,



2. Heat Flux

$$q_{\text{cond}} = \langle \tilde{T}_e \tilde{v}_r \rangle = - \sum_k \frac{k_y}{B} |\tilde{T}_{e,k}| |\tilde{\Phi}_k| \gamma_{T_e \phi} \sin \theta_{T_e \phi}$$

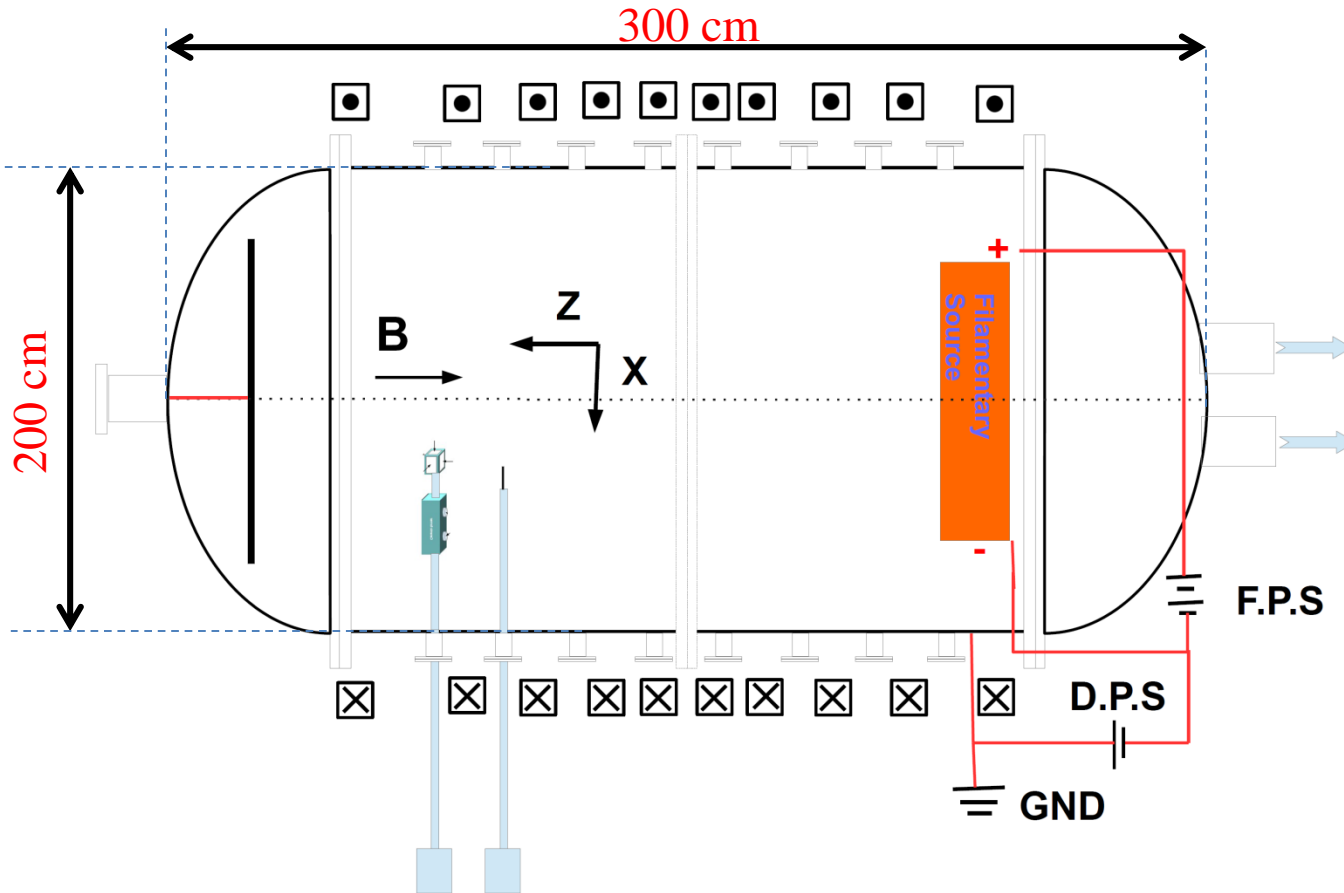
$$\eta_e > \frac{2}{3} \left(\frac{L_n}{L_{Te}} \right) \Omega_{ci} < \omega \ll \Omega_{ce},$$

$$\gamma_{ETG} = \left(\frac{\sqrt{3}}{2} \right) \left[\frac{\eta_e \omega_{*e} k_z^2 c_e^2}{\tau_e} \right]^{1/3}$$

$$k_\perp \rho_e \leq 1 < k_\perp \rho_i, \frac{\omega}{k_\perp} \geq c_i$$



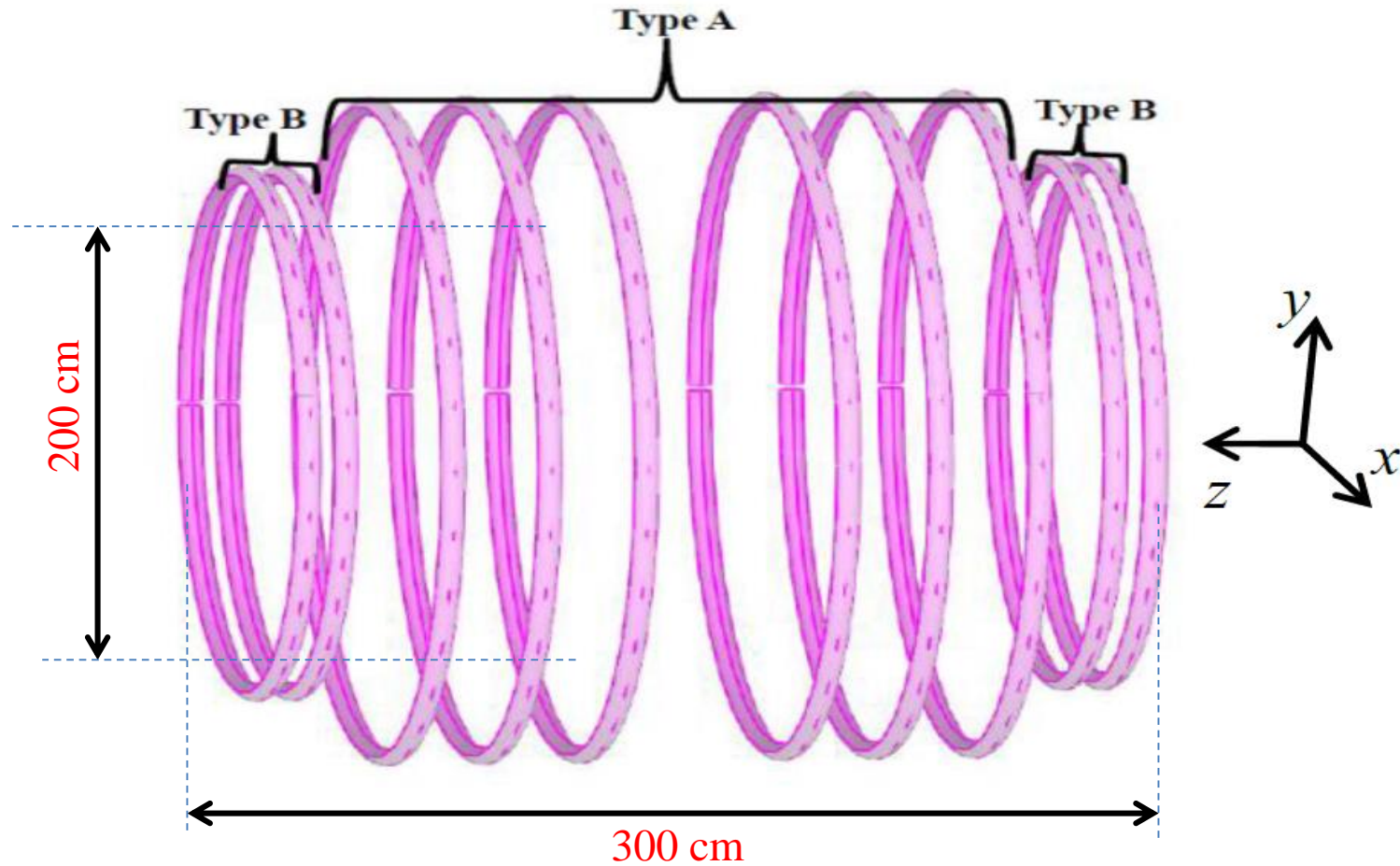
Experimental setup





Experimental setup

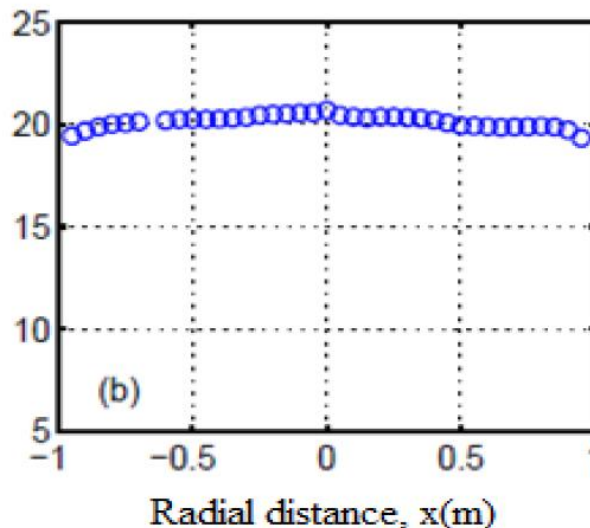
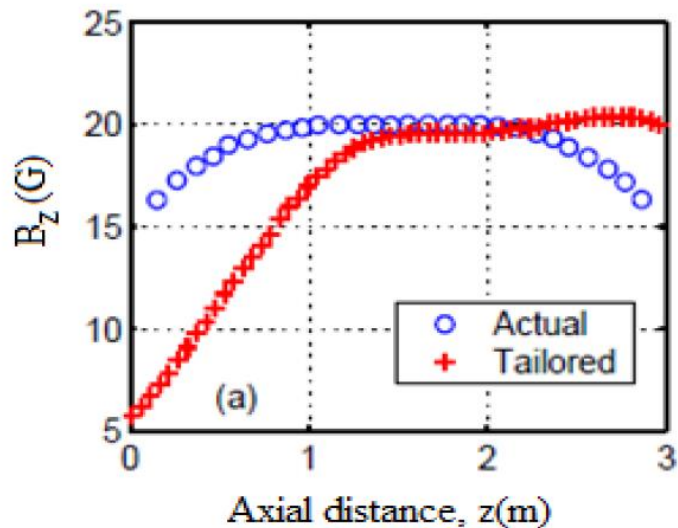
- Coil arrangement for axial magnetic field (B_z)



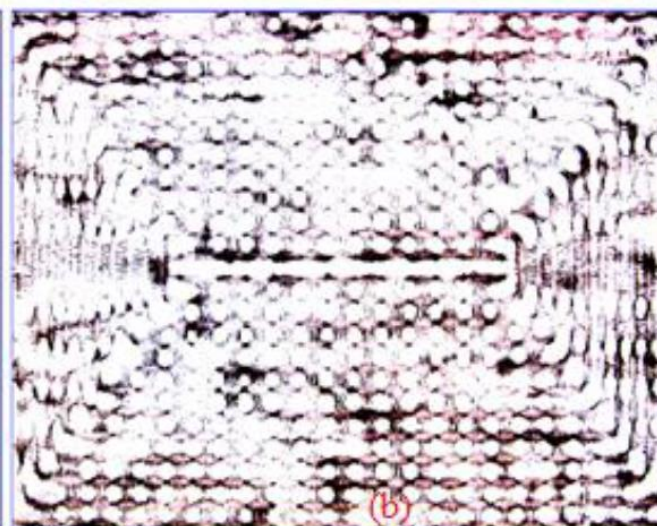
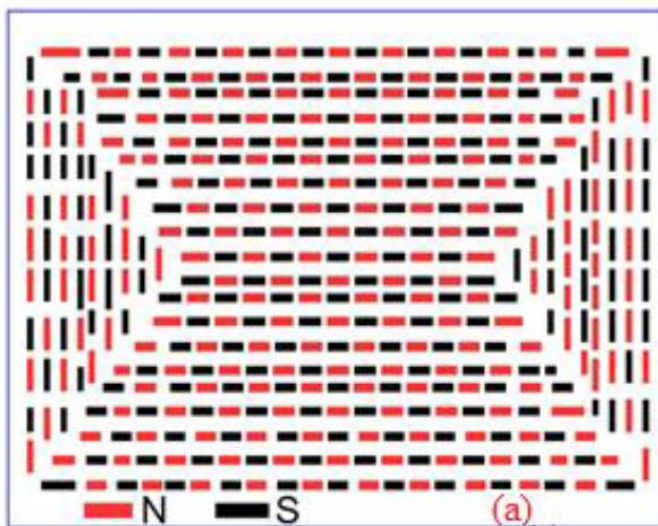


Experimental setup

Radial confinement

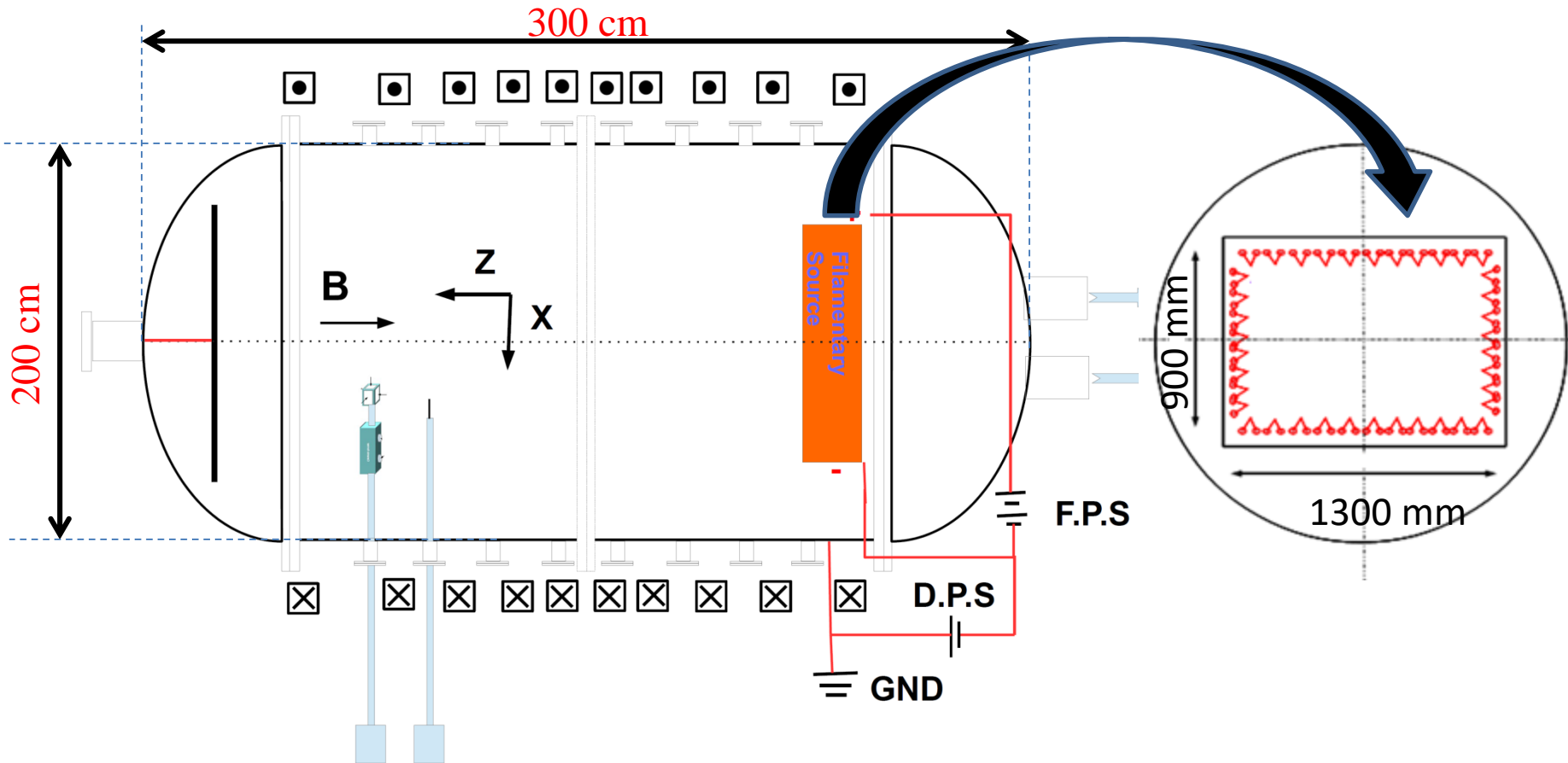


Axial confinement



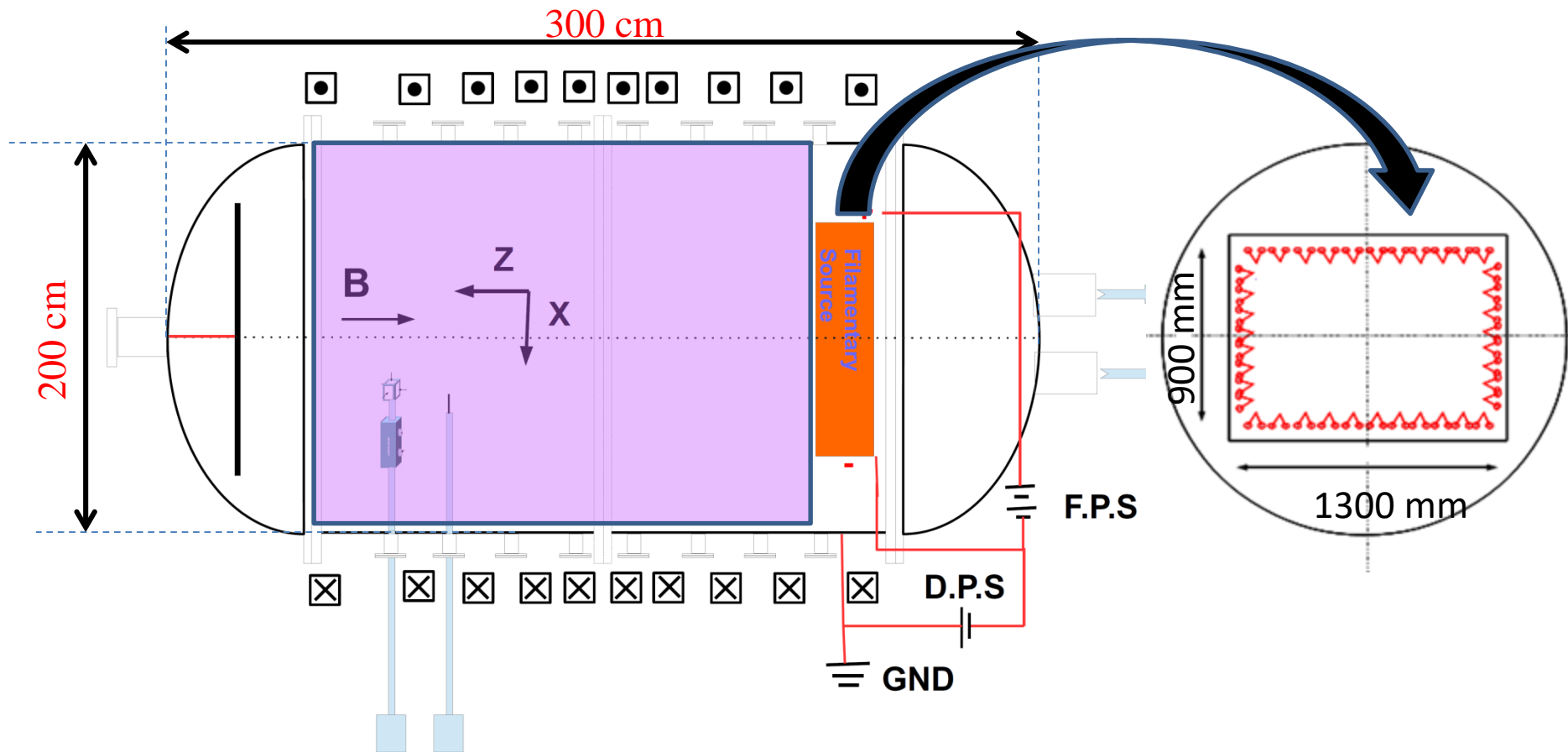


Experimental setup





Experimental setup





Experimental setup

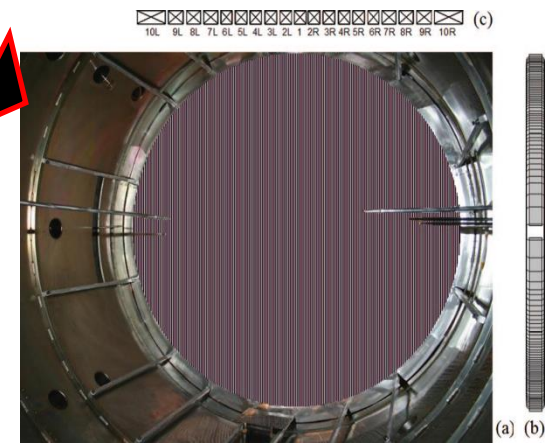
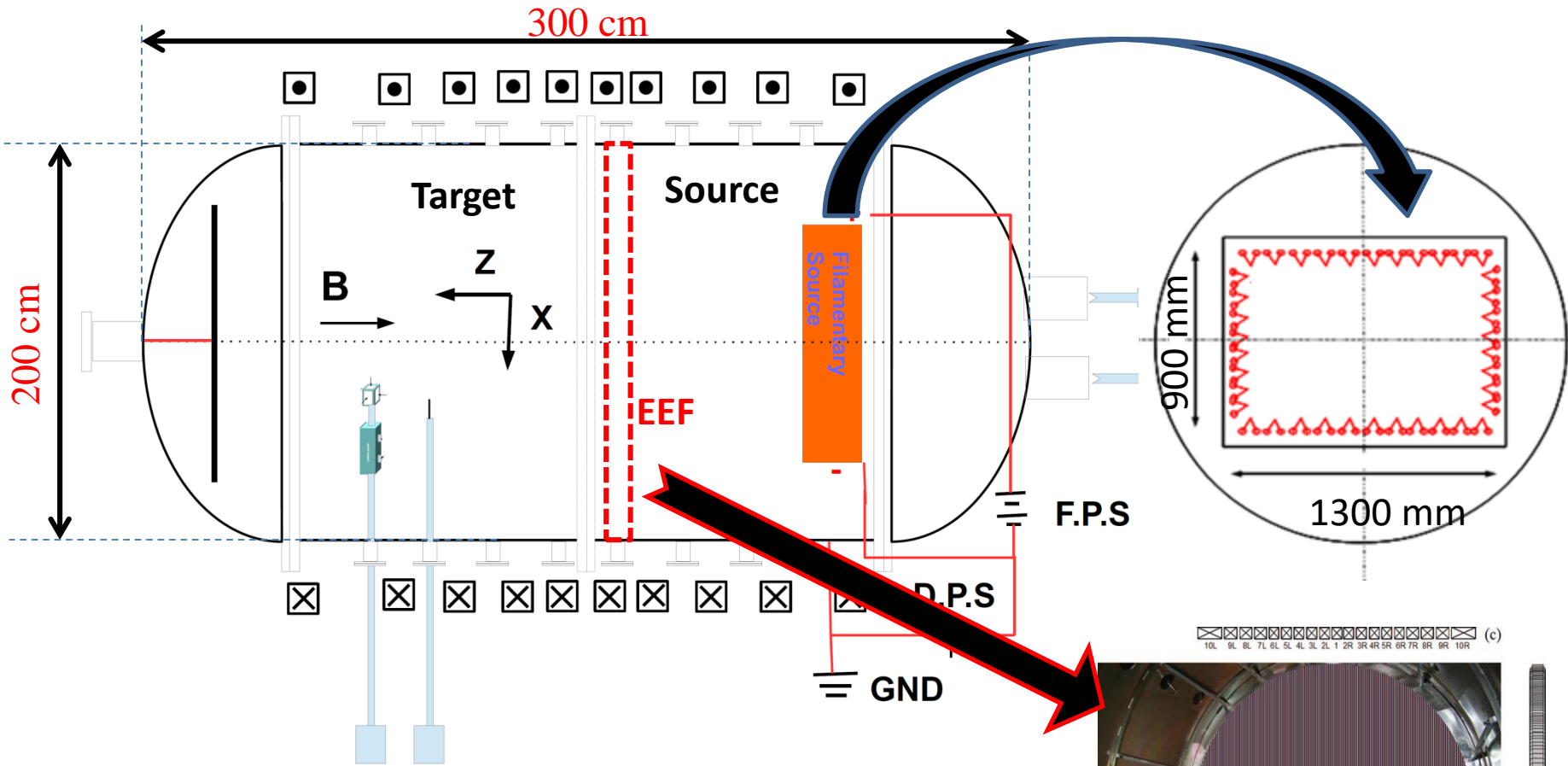
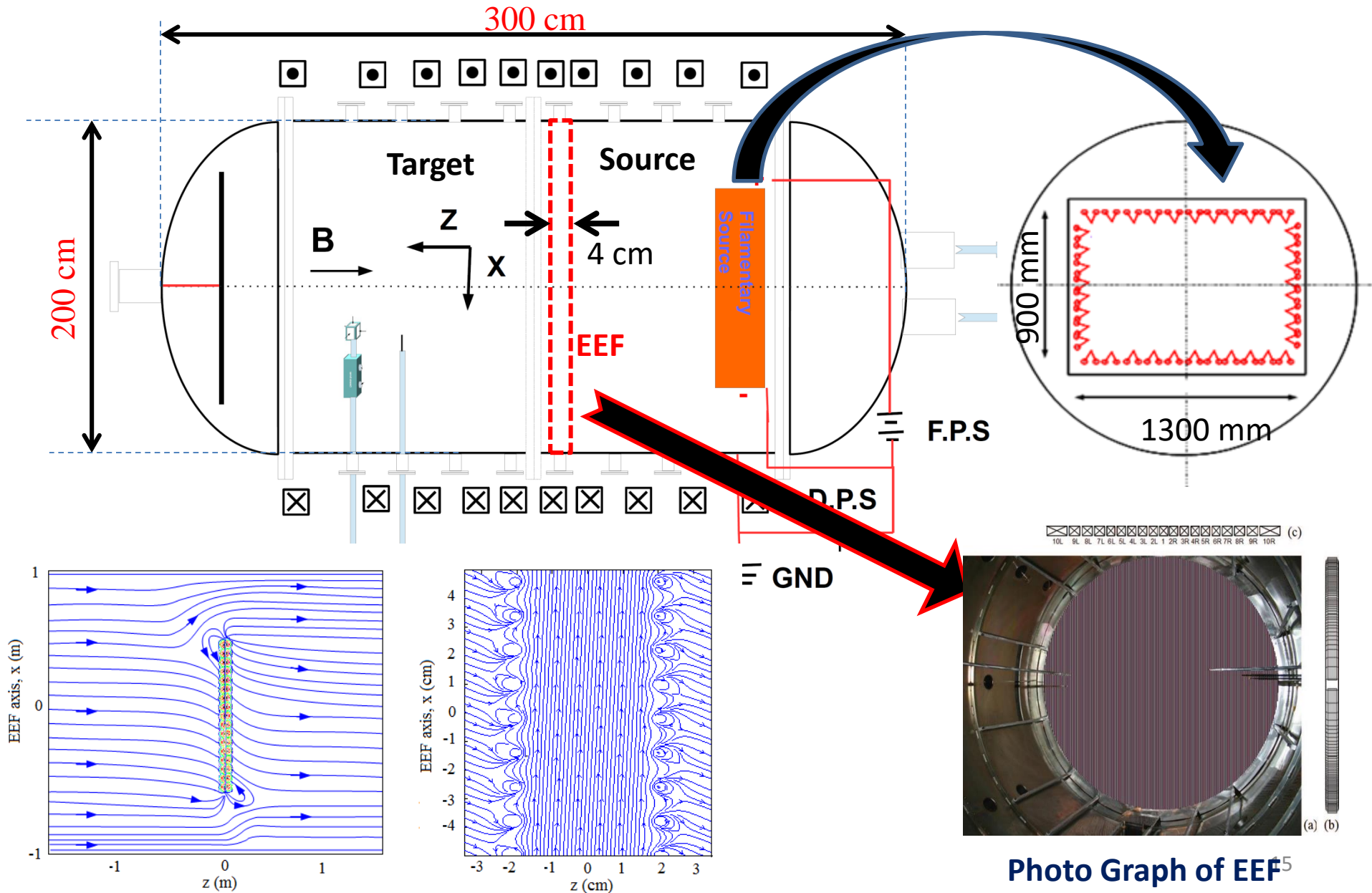


Photo Graph of EEF^{#4}



Experimental setup





Experimental setup

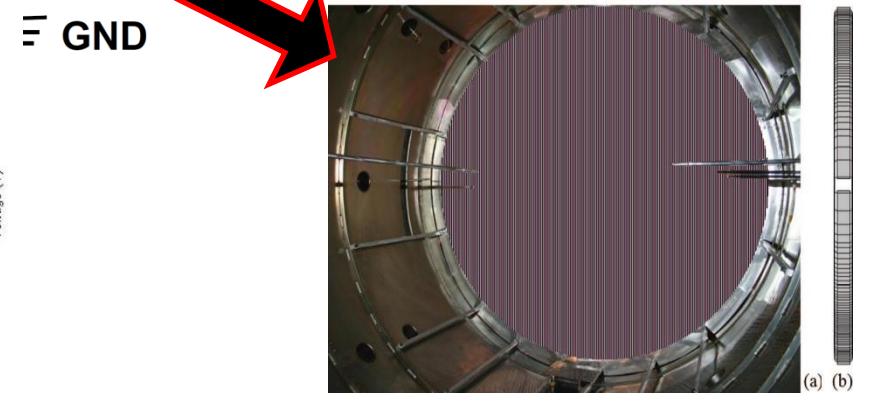
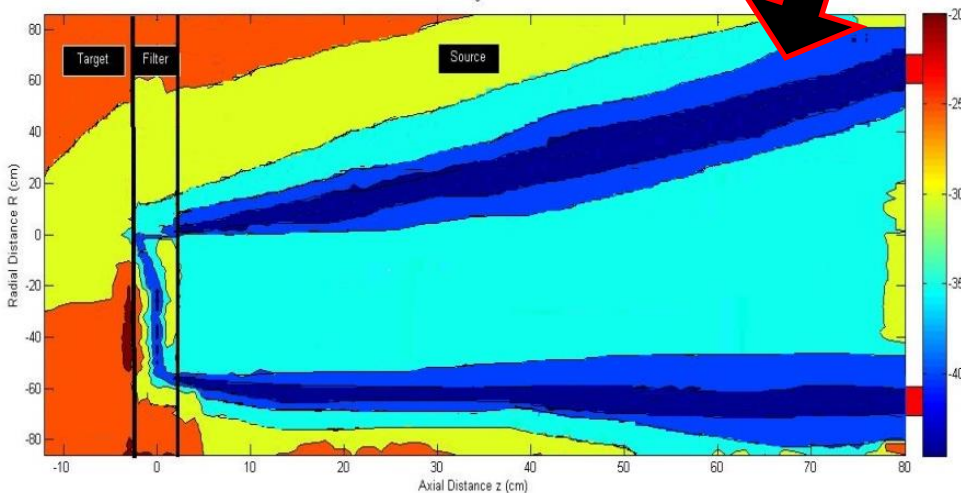
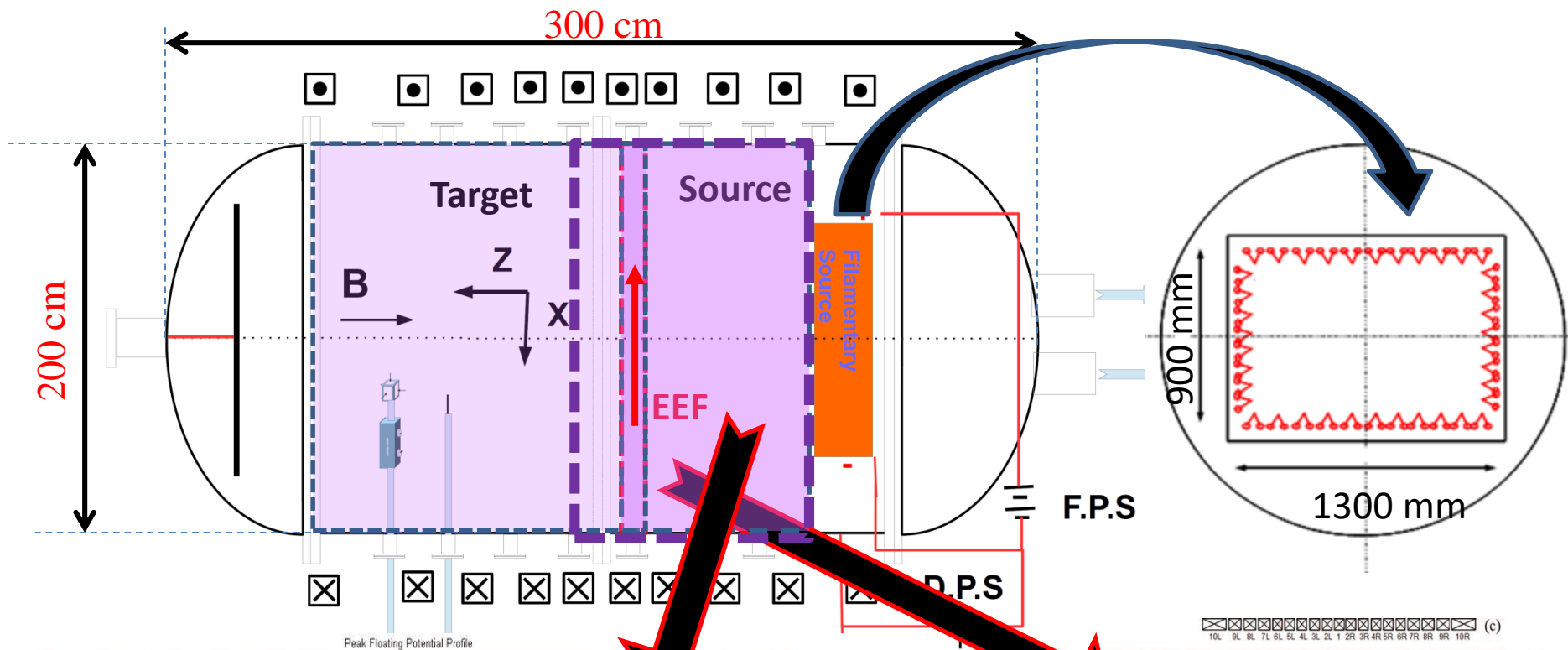
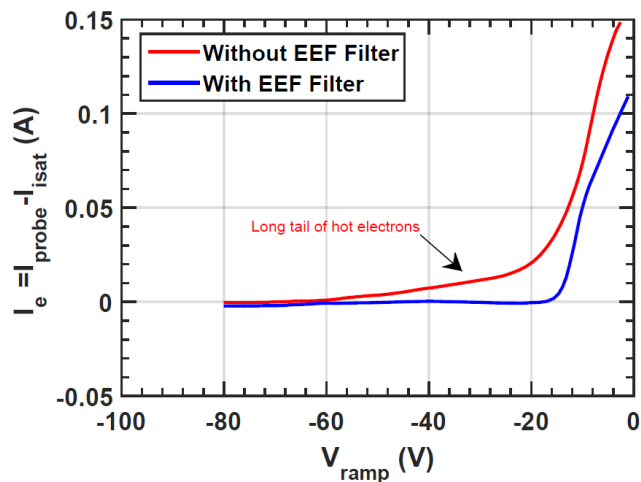
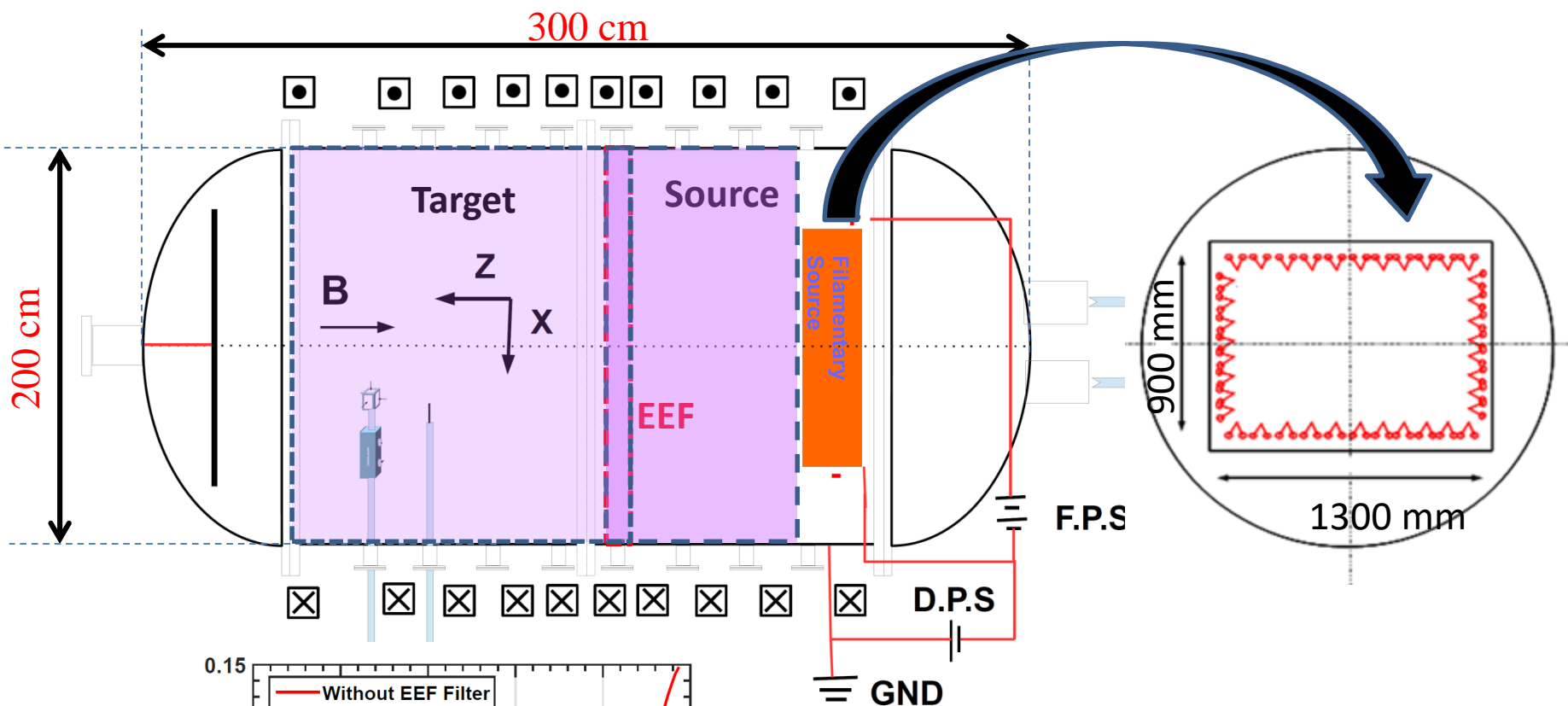


Photo Graph of EEF⁶



Experimental setup



Applied magnetic field, B_z	6.0 G
EEF magnetic field, B_{EEF}	160 G
Discharge current, I_D	~150-400 A
Pulse duration Δt_{pulse}	9.2 ms
Neutral Pressure, P_{Ar}	4×10^{-4} (mbar)



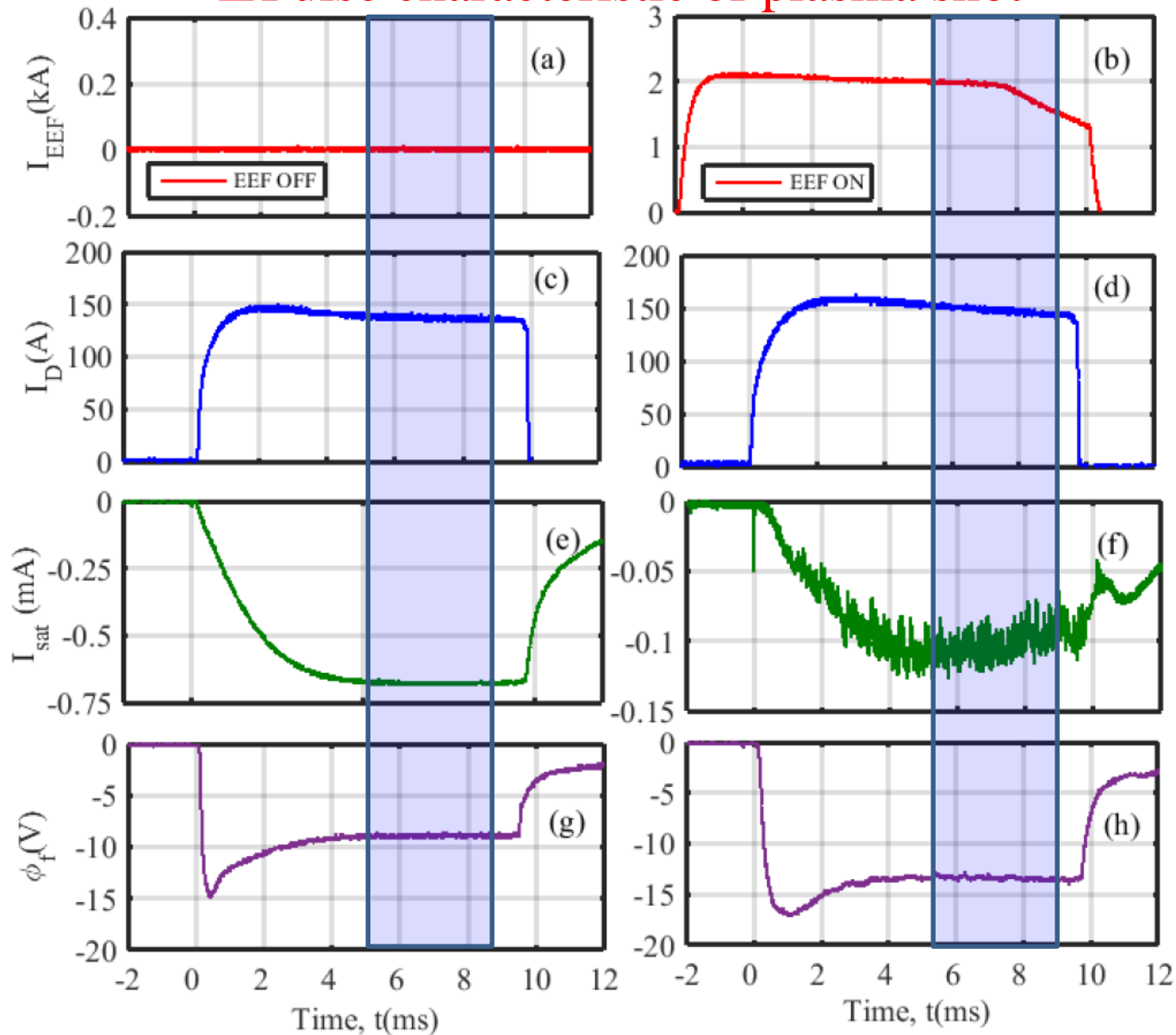
Experimental plasma parameters

	Source	EEF	Target
Plasma density, $n_e(\text{cm}^{-3})$	6.0×10^{11}	2.3×10^{11}	1×10^{11}
Electron temperature, $T_e(\text{eV})$ & $T_i = T_e/10$	8.0	2.5	2.2
Plasma beta, β	1.6	10^{-3}	0.2
f_{pe}	7×10^9	4.9×10^9	3.5×10^9
f_{pi}	3×10^7	1.8×10^7	1.3×10^7
f_{ce}	1.0×10^7	2.8×10^8	1.0×10^7
f_{ci}	236	6×10^3	236
Debye length, $\lambda_{De}(\text{cm})$	2.1×10^{-3}	2.3×10^{-3}	2.7×10^{-3}
Electron gyro-radius, $\rho_e(\text{cm})$	0.8	0.02	0.5
Ion gyro-radius, $\rho_i(\text{cm})$	73	2.2	46



Experimental Investigations on ETG

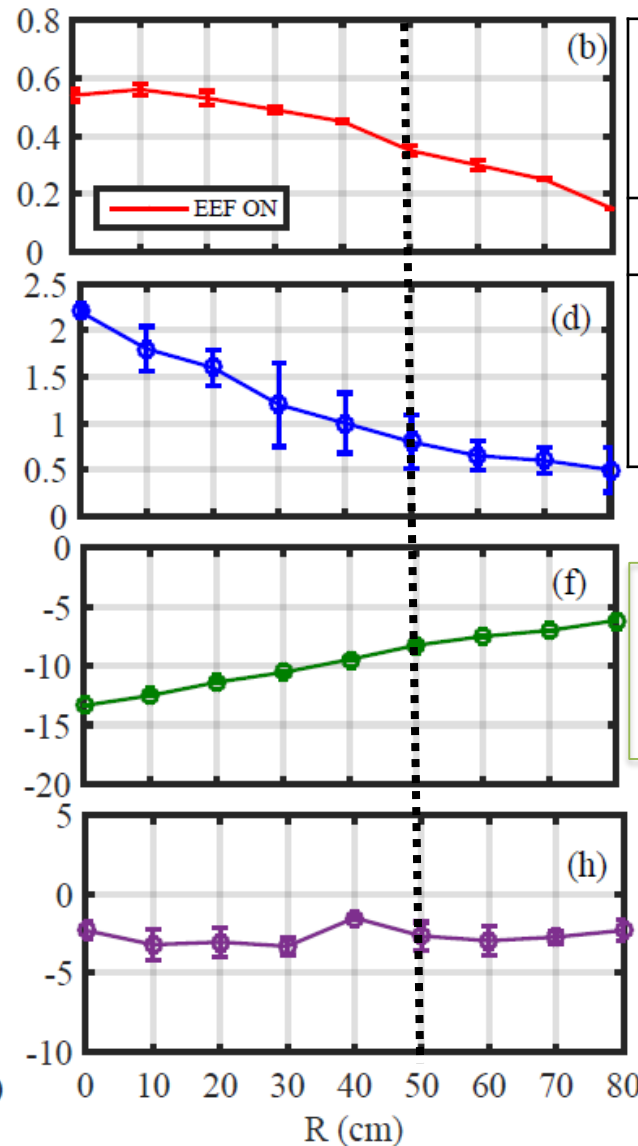
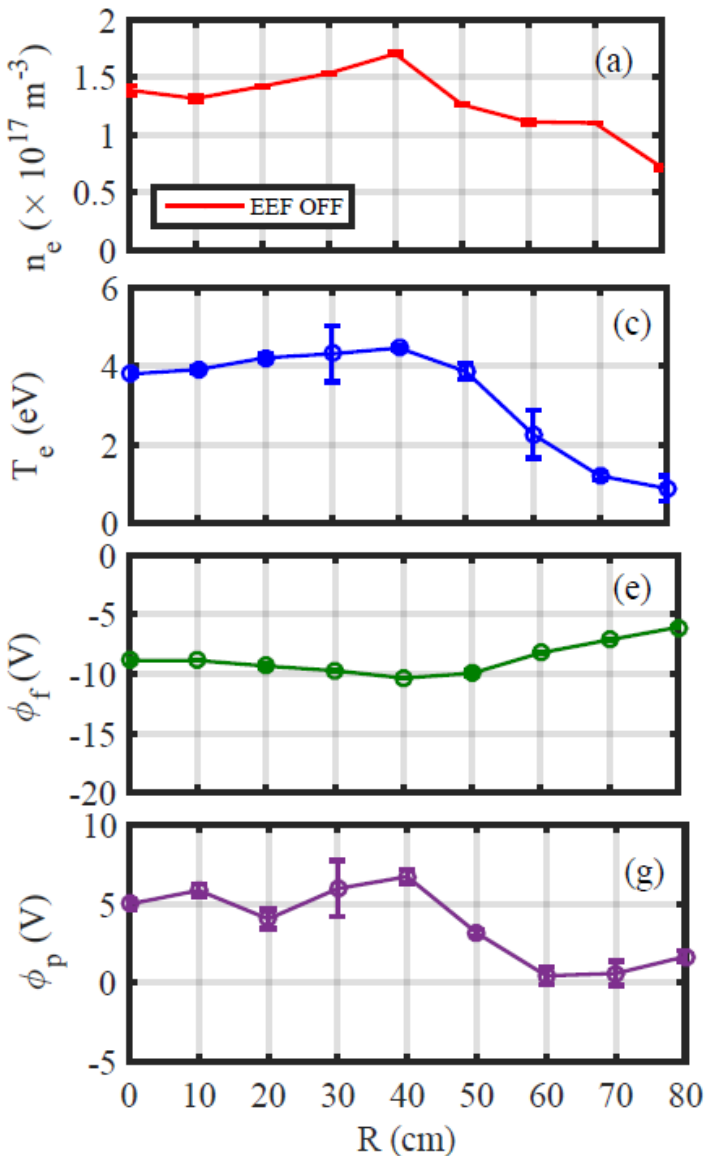
□ Pulse characteristic of plasma shot





Experimental Investigations on ETG

□ Mean plasma profile



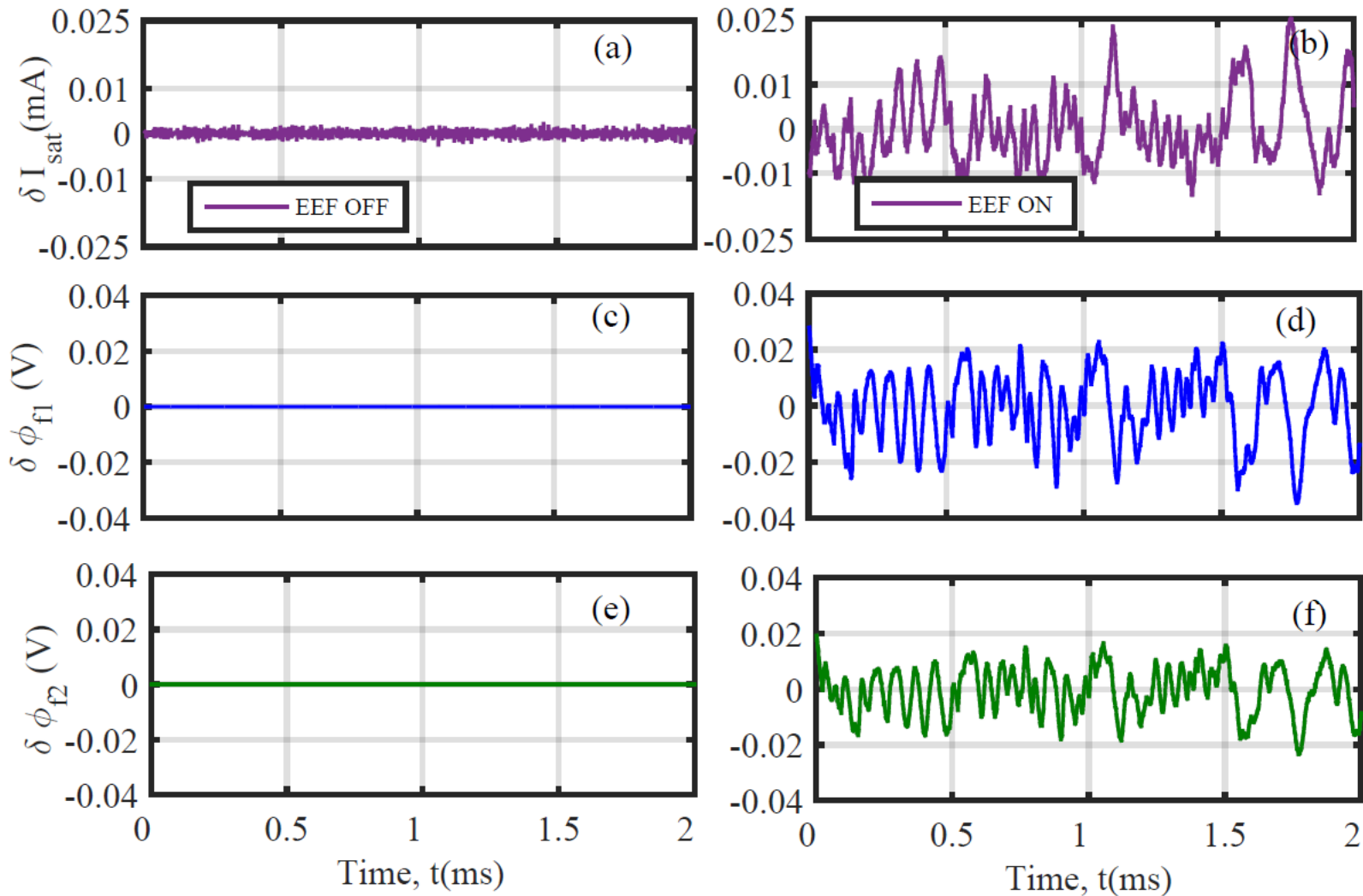
EEF OFF (0 -50 cm)	EEF ON (0 -50 cm)
$L_n \approx 400\text{cm}$	$L_n \approx 300\text{cm}$
$L_{Te} \approx 650$	$L_{Te} \approx 55\text{cm}$

□ $\eta_e > \frac{2}{3}$ for EEF ON case,
ETG threshold condition is
satisfied



Experimental Investigations on ETG

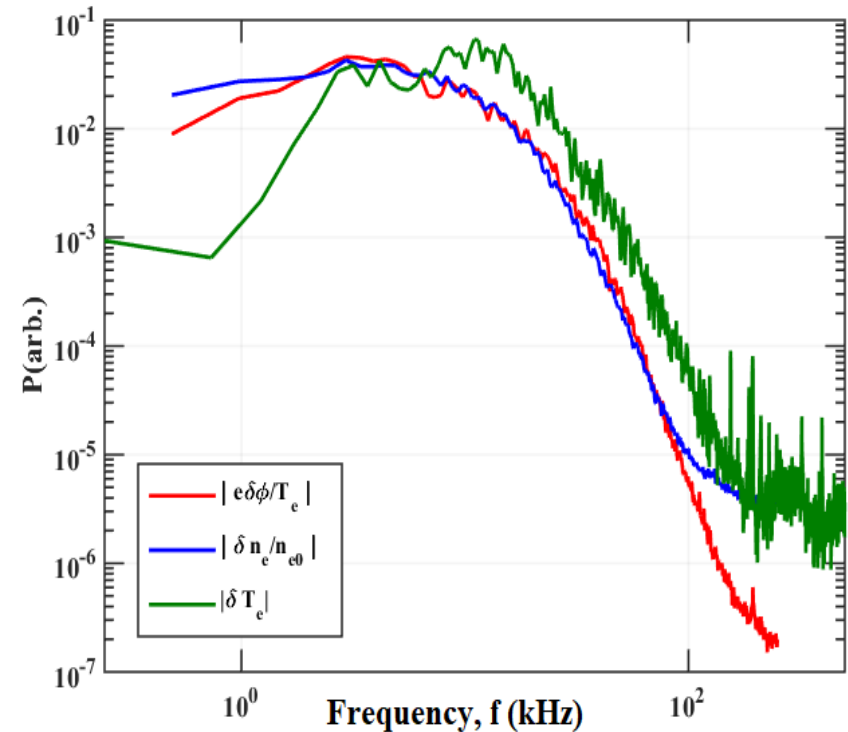
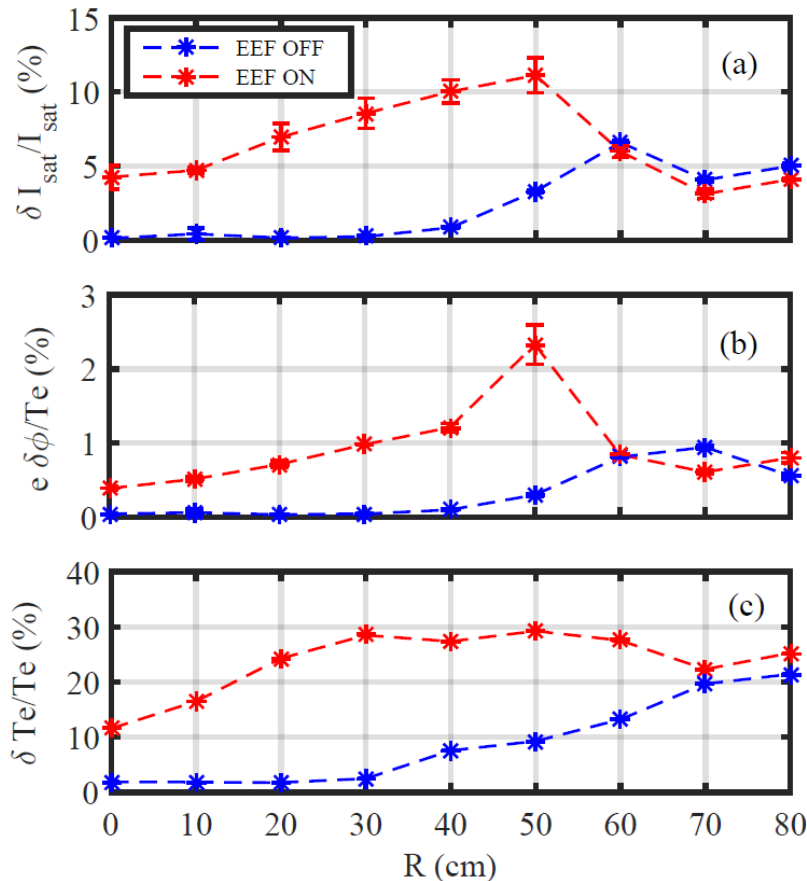
□ Temporal Evolution of Fluctuation





Experimental Investigations on ETG

Radial Profile of fluctuation and Power Spectra of fluctuation

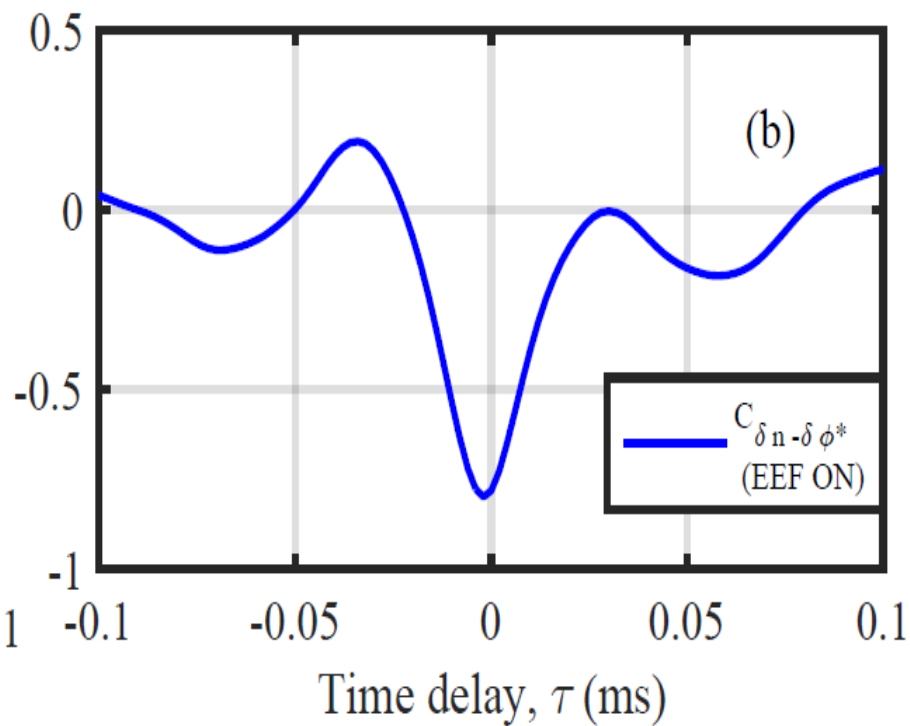
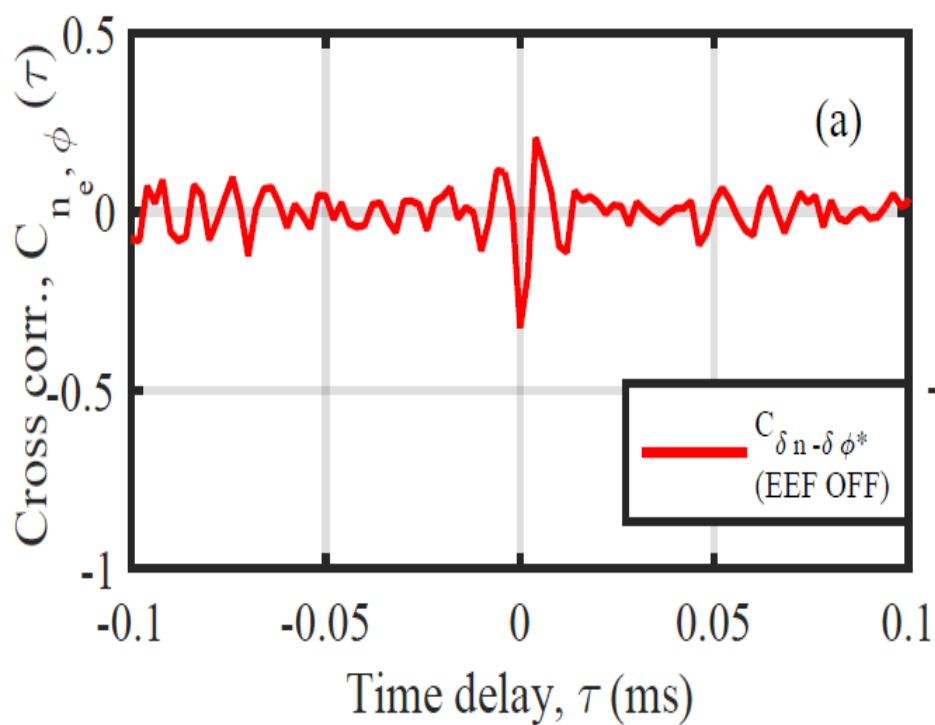


- Fluctuation enhances when EEF is ON in the core
- Density and Potential fluctuation share common frequency band of spectrum



Experimental Investigations on ETG

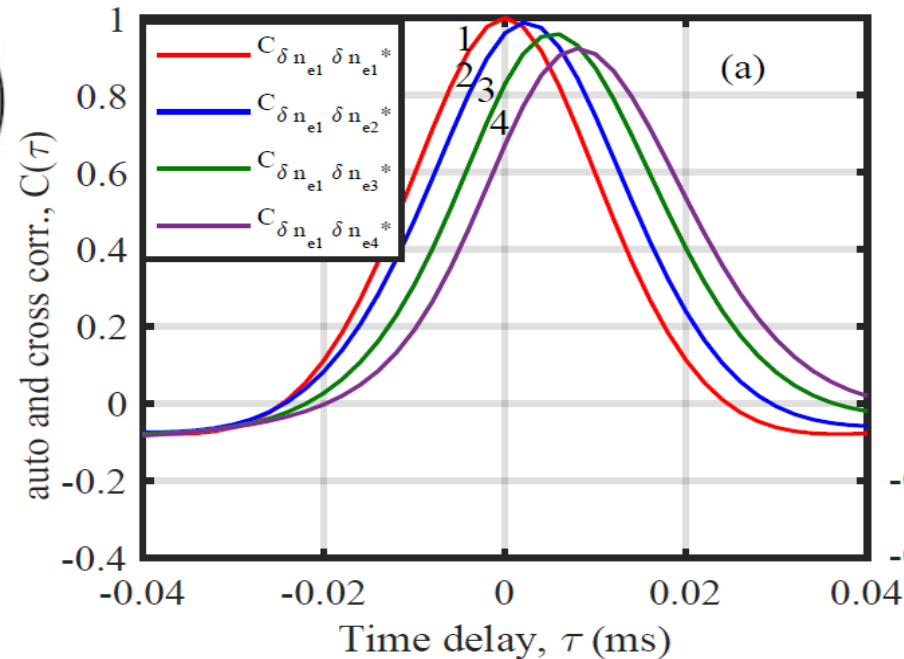
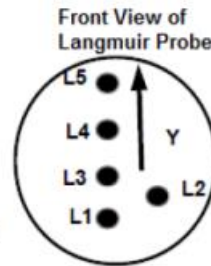
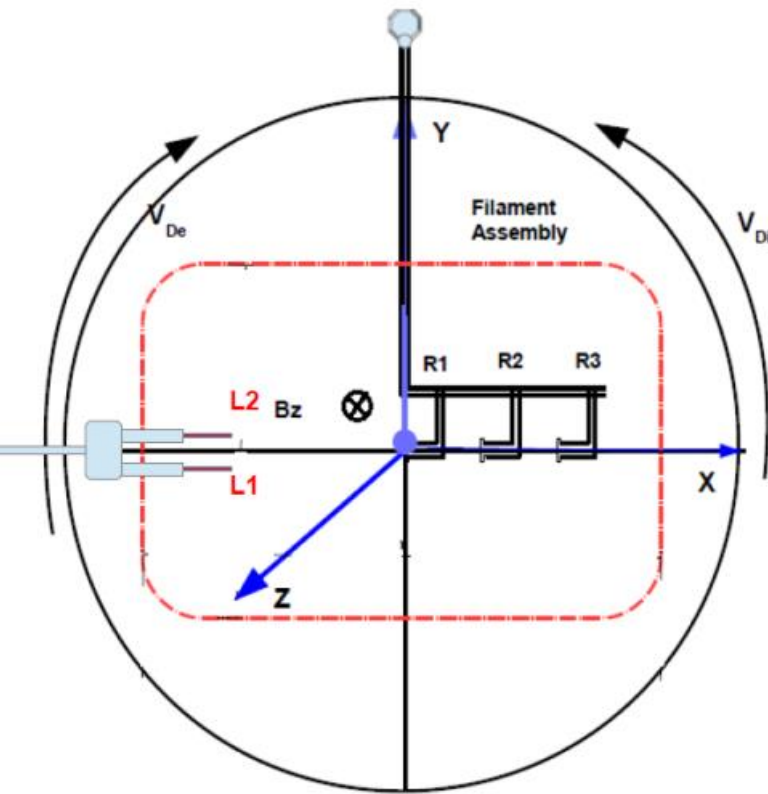
□ Correlation between \tilde{n} and $\tilde{\phi}$





Experimental Investigations on ETG

□ Diamagnetic Drift Direction and Poloidal Rotation of the mode



- ✓ Mode propagation is in positive y -direction, similar to V_{di}
- ✓ Measured poloidal propagation velocity, $V_{\theta} = 2.5 \times 10^3 \text{ m/sec}$



Experimental Investigations on ETG

□ Characterization of ETG turbulence

$$\eta_e = \frac{L_n}{L_{Te}} > \frac{2}{3}, \frac{k_z}{k_\perp} \ll 1$$

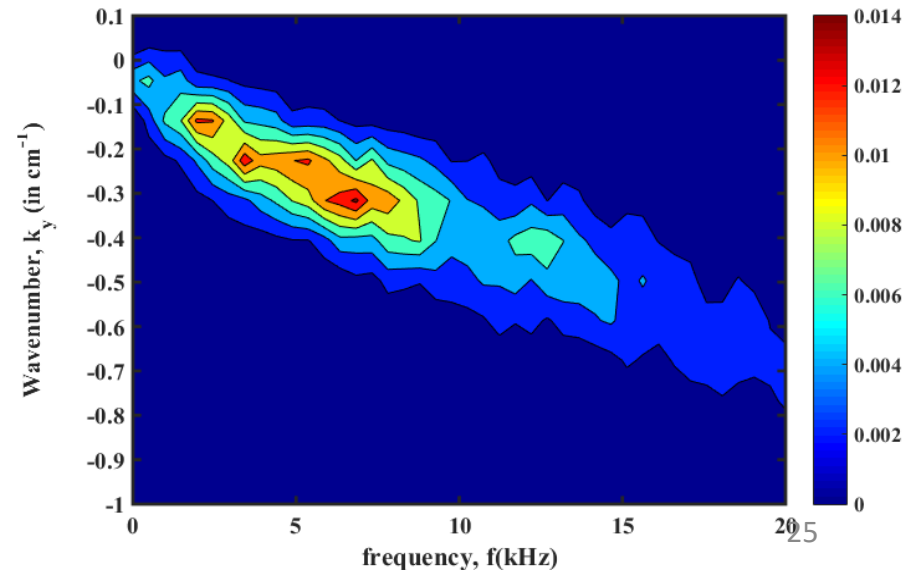
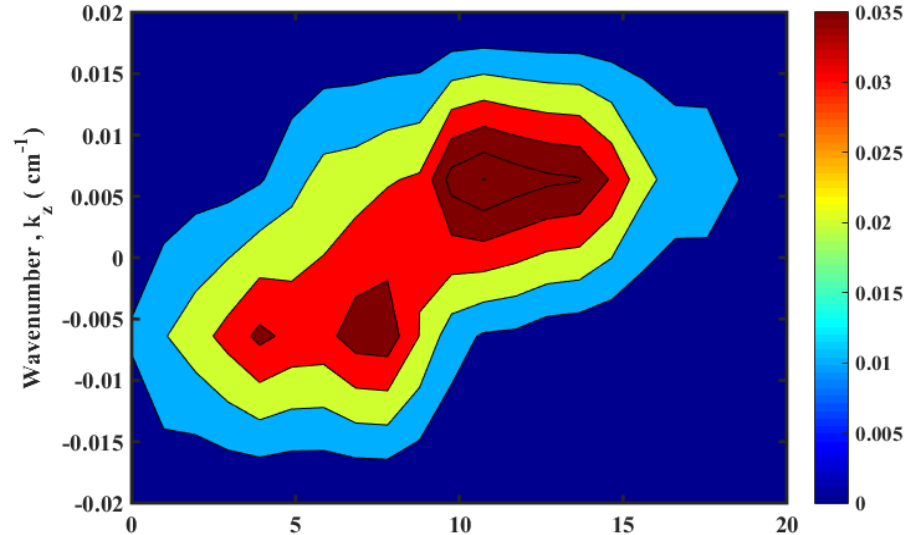
1. Frequency ordering
($v_{in}(3 \times 10^3 s^{-1}) < \omega$)

$$\Omega_{ci}(1.5 \text{ krad/sec}) < \omega(6 - 100 \text{ krad/sec}) \ll \Omega_{ce}(10^3 \text{ krad/sec})$$

2. Wavelength ordering
($\rho_e \approx 0.5 \text{ cm}$ and $\rho_i \approx 40 \text{ cm}$)
 $k_\perp \rho_e \leq 1, \quad k_\perp \rho_i > 1$

3. Density and potential fluctuations

$$\tilde{n} = -\tau_e^* \tilde{\phi}$$





Theoretical Understanding of slab ETG

□ Electron Dynamics

Continuity Equation

$$\frac{\partial n_e}{\partial t} + \nabla \cdot (n_e v_{e\perp}) + \nabla_{\perp} (n_e v_{ez}) = 0$$

Momentum Equation

$$\begin{aligned} m_e n_e \left(\frac{\partial v_e}{\partial t} + v_e \cdot \nabla v_e \right) \\ = e n_e \nabla_{\perp} \phi - \nabla p_e - e n_e \frac{v_e \times B_z}{c} \\ - m_e n_e v_{en} v_e \end{aligned}$$

Energy Equation

$$\frac{3}{2} n_e \frac{dT_e}{dt} + p_e \nabla \cdot v_e = -\nabla \cdot q_e^*$$

Electron drift can be following terms

$$v_{e\perp} = (v_E + v_{*pe}) \left(1 - \frac{\delta B_z}{B_z} \right) + v_{pe} + v_{\pi}$$

□ Ampere's Law

$$\nabla \times B = \frac{4\pi}{c} j \approx \frac{4\pi e n_e}{c} v_e$$

□ Ion dynamics

Continuity Equation

$$\frac{\partial n_i}{\partial t} + \nabla \cdot (n_i v_{i\perp}) = 0$$

Momentum Equation

$$m_i n_i \left(\frac{\partial v_i}{\partial t} + v_i \cdot \nabla v_i \right) = -e n_i \nabla_{\perp} \phi - T_i \nabla_{\perp} n_i$$

□ ETG model equations;

$$\tilde{n}_i = -\tau_e^* \tilde{\phi}$$

$$\tilde{T}_e = \left[\left(\frac{1}{L_{Te}} - \frac{2}{3} \frac{1}{L_n} \right) \frac{k_y \rho_e c_e}{\omega} - \frac{2}{3} \tau_e^* \right] \tilde{\phi}$$

$$\tilde{B} = \hat{\beta} \left[\left(1 + \frac{5}{3} \tau_e^* \right) - \left(\frac{1}{L_{Te}} - \frac{2}{3} \frac{1}{L_n} \right) \frac{k_y \rho_e c_e}{\omega} \right] \tilde{\phi}$$

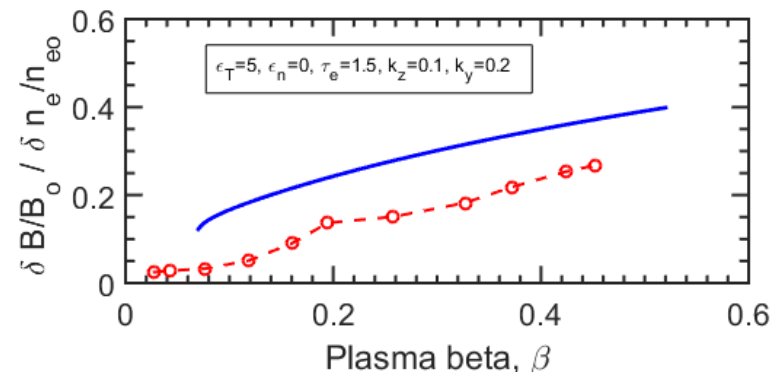
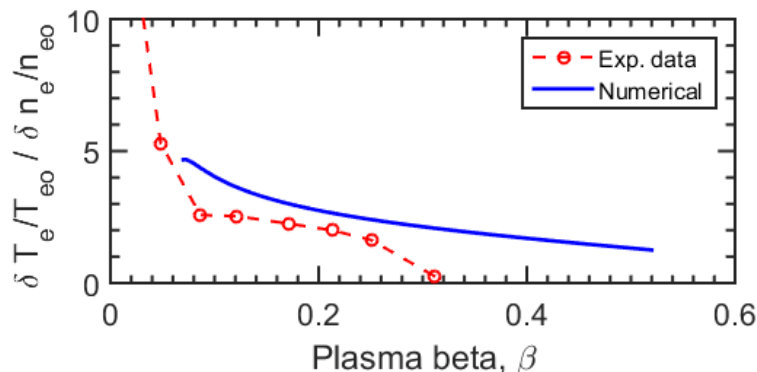
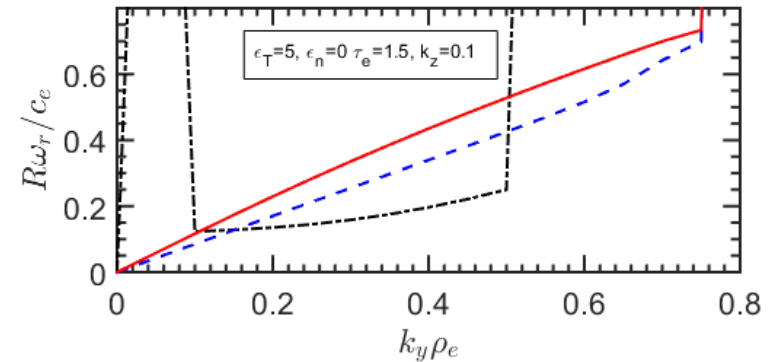
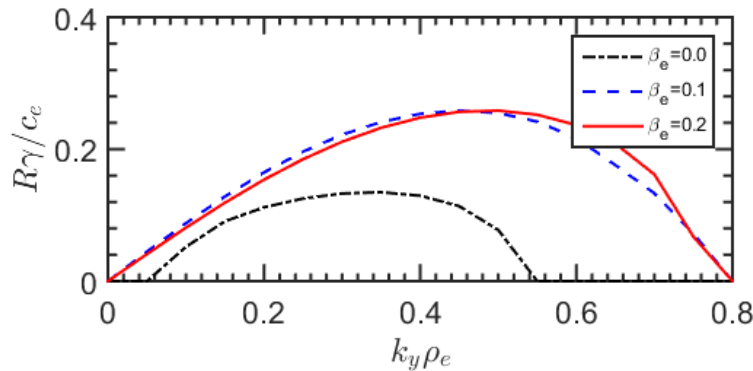


Theoretical Understanding of slab ETG

Numerical Solution of W-ETG dispersion relation and comparison with experimental data

$$\omega \left[\omega \tau^* + \omega_{*e} + k_{\perp}^2 \rho_e^2 (\omega - \omega_{*pe}) + \frac{\beta_e}{2} (1 + \tau_e^*) (\omega - \omega_{*pe}) \right] - \frac{\beta_e}{2} (\omega - \omega_{*pe}) \left[\left(\eta_e - \frac{2}{3} \right) \omega_{*e} - \frac{2}{3} \tau_e^* \omega \right]$$

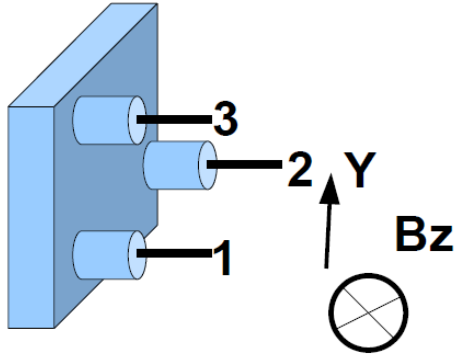
$$= k_z^2 c_e^2 k_{\perp}^2 \rho_e^2 \left[\frac{(1 + \tau_e) \omega - \left(\eta_e - \frac{2}{3} \right) \omega_{*e} + \frac{2}{3} \tau_e^* \omega}{\left\{ \omega \left(\frac{\beta_e}{2} + k_{\perp}^2 \rho_e^2 \right) + i v_e k_{\perp}^2 \rho_e^2 \right\} - \frac{\beta_e}{2} \omega_{*pe}} \right]$$





I. Study of electrostatic particle flux

Flux Probe Assembly and Fluctuation Measurement



The 3-pin LP assembly is used for measuring turbulent particle flux

Particle flux can be estimated as

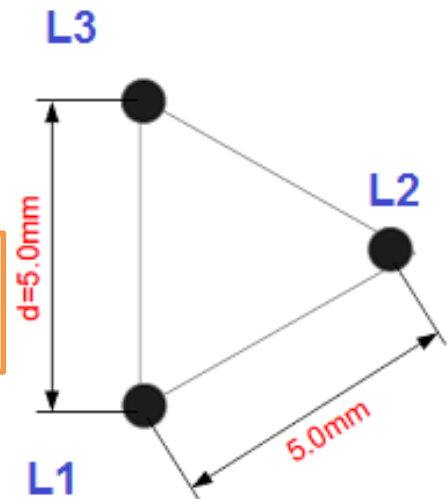
$$\tilde{\Gamma}_{es} = \tilde{n} \cdot \tilde{v}_r$$

Where \tilde{v}_r , radial velocity fluctuation given by

$$\tilde{v}_r = \frac{\tilde{E}_\theta \times \vec{B}}{B_0^2}; \tilde{E}_\theta \text{ is measured with floating}$$

potential fluctuation measurement with poloidally separated Langmuir probes

$$\tilde{E}_\theta = -\frac{(\tilde{\phi}_3 - \tilde{\phi}_1)}{d}$$

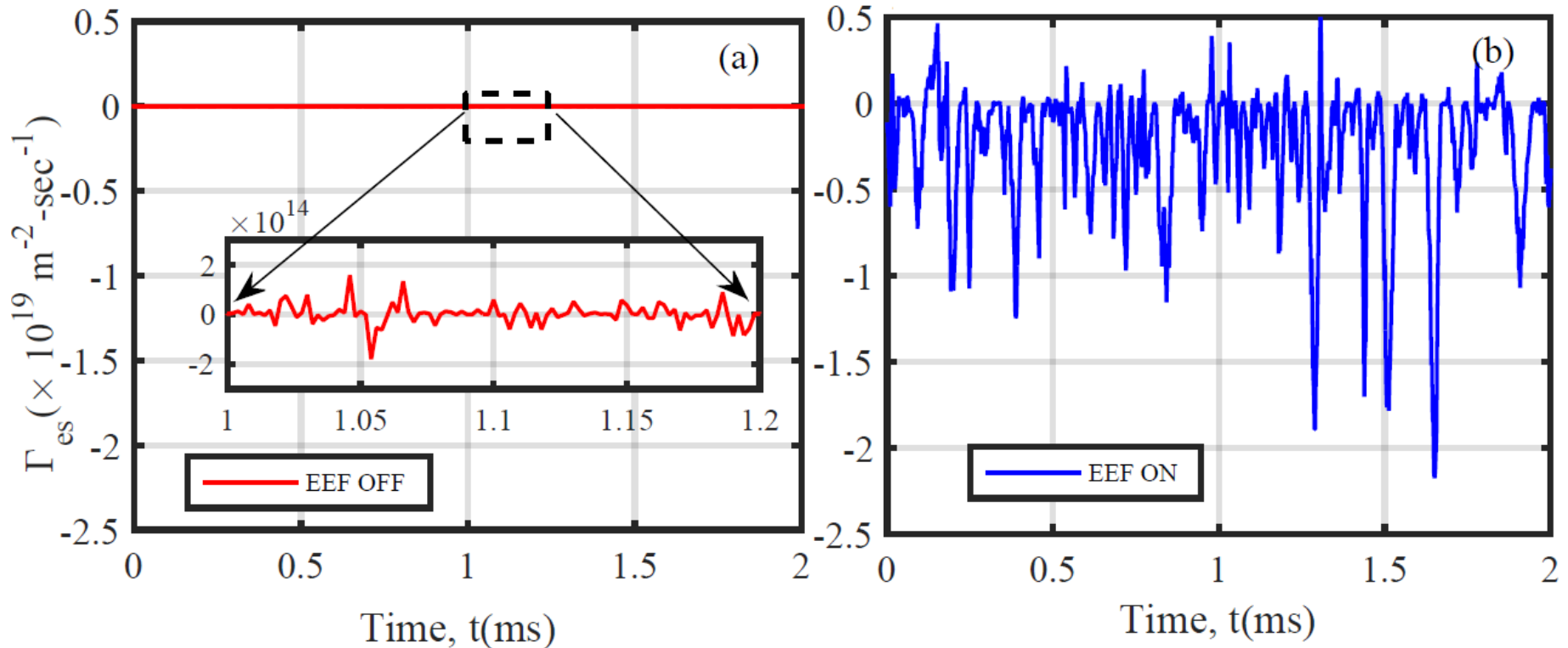


Schematic of Langmuir Probe for flux measurement



I. Study of electrostatic particle lux

□ Particle flux, Γ_{es} measurement

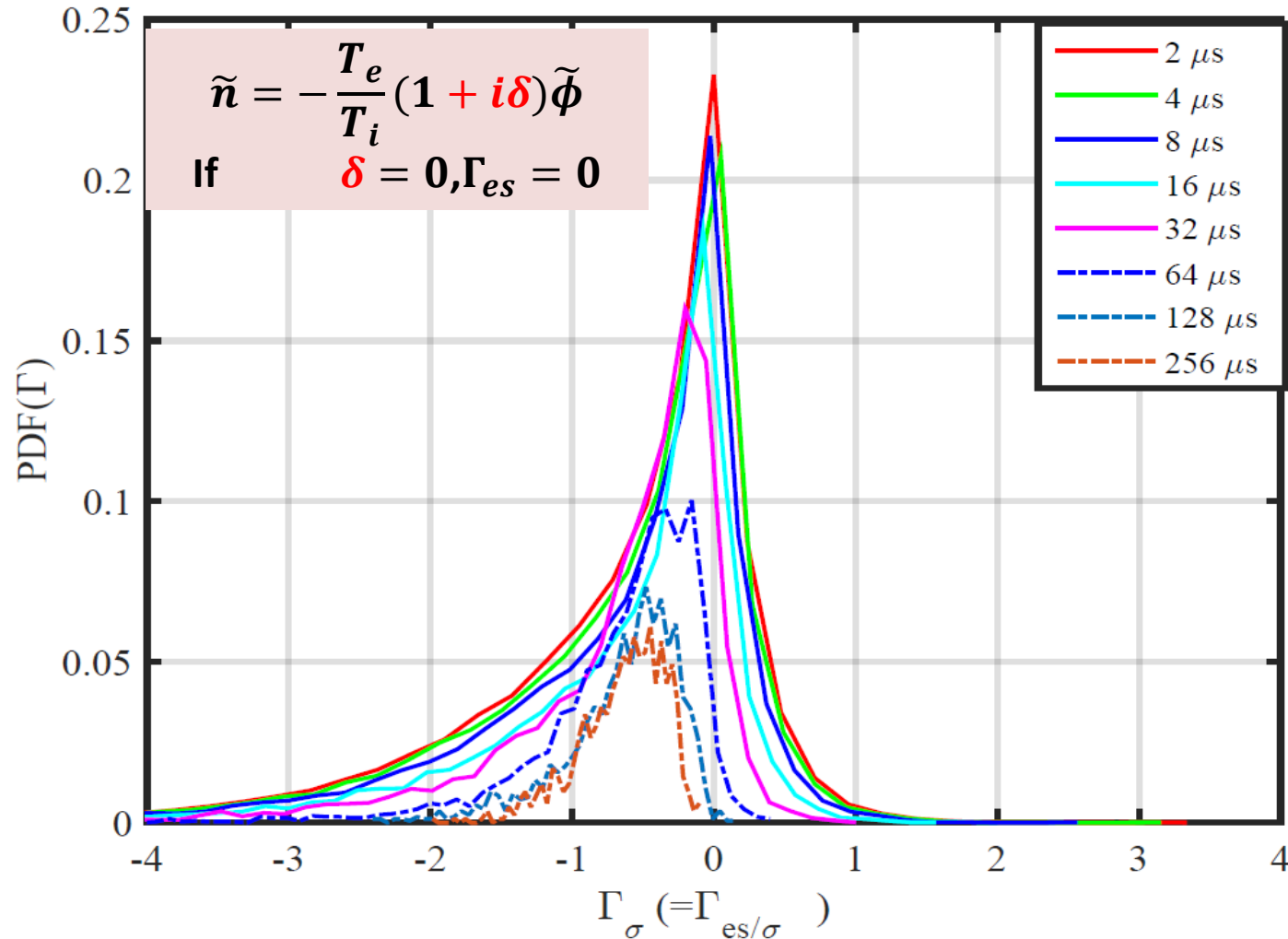


Particle flux for (a) EEF OFF and (b) EEF ON case is shown. The flux is enhanced in EEF ON case and is prominently negative. In EEF OFF plasma insignificantly low level of flux is observed.



I. Study of electrostatic particle flux

Probability Distribution Function (PDF)



Probability distribution function (PDF) for particle flux (Γ_{es}), in the units of standard deviation ($\sigma_{\Gamma_{es}} \approx 4 \times 10^{18} m^{-2} sec^{-1}$) for different averaging time. The distribution of particle flux is asymmetric.



I. Study of electrostatic particle flux

□ Recalculation of ion response on ETG mode

- By considering un-magnetized and collision-less ion in ETG dynamics , where $k_{\perp} V_{thi} \sim |\omega|$, ETG mode resonates with background ions, which results in deviation of ions from Boltzmann condition.
- This response of ions can be determined by drift kinetic equation as follows;

$$\frac{\partial \tilde{f}_i}{\partial t} + \vec{V}_{\perp} \cdot \frac{\partial \tilde{f}_i}{\partial \vec{x}} + \frac{Ze}{m_i} \delta E_{\perp} \cdot \frac{\partial f_{oi}}{\partial \vec{V}} = 0 \dots \dots \dots (1)$$

Assuming Maxwellian equilibrium distribution function for ions in one dimension,

$$f_{oi} = n_{io} \sqrt{\frac{m_i}{2\pi T_i}} \exp\left(-\frac{V_y^2}{V_{thi}^2}\right) \dots \dots \dots (2)$$

Where $V_{thi}^2 = \frac{2T_i}{m_i}$, using above distribution for ion in equation (1), we get fluctuating ion distribution as

$$\tilde{f}_i = -\tau_e \tilde{\phi} \frac{V_y}{V_y - \frac{\omega}{k_y}} f_{oi} \dots \dots \dots (3)$$

Then the ion density fluctuation

$$\tilde{n}_i = \frac{1}{n_{io}} \int \tilde{f}_i dV_{\perp}$$

$$\tilde{n}_{io} = -\frac{\tau_e \tilde{\phi}}{\pi^{\frac{1}{2}} V_{thi}} \int dV_y \frac{V_y}{V_y - \frac{\omega}{k_y}} \exp\left(-\frac{V_y^2}{V_{thi}^2}\right) \dots \dots \dots (4)$$



I. Study of electrostatic particle flux

Re-writing equation (4)

$$\tilde{n}_i = -\frac{\tau_e \tilde{\phi}}{\pi^{1/2}} \int d\xi \frac{\xi}{\xi - \hat{\omega}} \exp(-\xi^2) \dots \dots \dots (5)$$

Where $\xi = V_y/V_{thi}$ and $\hat{\omega} = \frac{\omega}{k_y V_{thi}}$

Simplifying equation (5), we have $\tilde{n}_i = -\tau_e \tilde{\phi} [1 + \hat{\omega} Z(\hat{\omega})] \dots \dots \dots (6)$

Where $Z(\hat{\omega})$ is known as Dispersion function and defined as $Z(\hat{\omega}) = \frac{1}{\pi^{1/2}} \int_{-\infty}^{\infty} \frac{e^{-\xi^2}}{(\xi - \hat{\omega})} d\xi$

For small ' $\hat{\omega}$ ',

$$Z(\hat{\omega}) = i\pi^{1/2} e^{-\hat{\omega}^2} - 2\hat{\omega} \left[1 - \frac{2\hat{\omega}^2}{3} + \dots \dots \dots \right] = i\pi^{1/2} e^{-\hat{\omega}^2} - 2\hat{\omega} + \dots \dots$$

Particle Flux; $\Gamma_{es} = \sum_{k_\theta} \frac{ik_\theta}{B} \tilde{n} \tilde{\phi}^*$, for slab geometry $k_\theta \sim k_y$. Using equation(6) and above expansion in flux expression, the part of particle flux becomes

$$\Gamma_{es} = \frac{k_y \hat{\omega}_r}{B} \tau_e \left[\frac{1}{\pi^{1/2}} e^{-\hat{\omega}_r^2} - 4\gamma \right] |\tilde{\phi}|^2 \dots \dots \dots (7)$$

For $\Gamma_{es} < 0$, $k_y \omega < 0$, ETG mode should propagate in Ion diamagnetic drift direction.



I. Study of electrostatic particle flux

We considered the ion non-adiabatic response by using kinetic approximation of ion dynamics perpendicular to static magnetic field, i.e.

$$\tilde{n} = -\frac{T_e}{T_i} \left[1 + \frac{i\pi^{1/2}\omega}{k_y v_{thi}} \exp\left(-\frac{\omega^2}{k_y^2 v_{thi}^2}\right) \right] \tilde{\phi} \dots\dots (A)$$

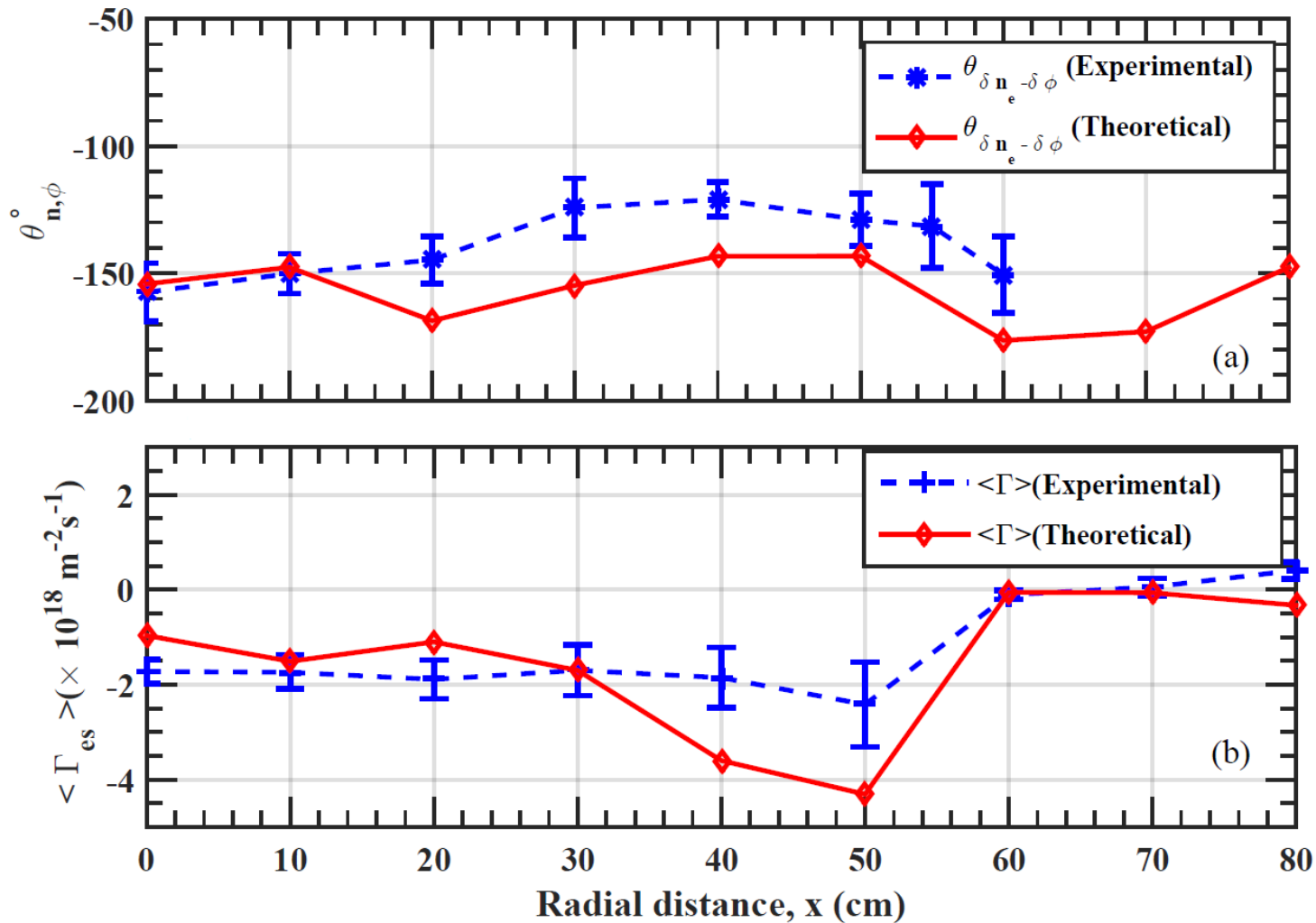
Using this relation the estimated particle flux is given by,

$$\Gamma_r = \langle \delta n \delta v_r \rangle = \sum_k \pi^{1/2} \frac{T_e}{T_i} n c_e k_y \rho_e \left(\frac{\omega_r}{k_\perp V_{thi}} \right) \left[\exp\left(-\frac{\omega_r^2}{k_\perp^2 V_{thi}^2}\right) \right] |\tilde{\phi}_k|^2 \dots\dots (B)$$

For $\Gamma_{es} < 0$, $k_y \omega < 0$, ETG mode should propagate in Ion diamagnetic drift direction.



I. Study of electrostatic particle flux

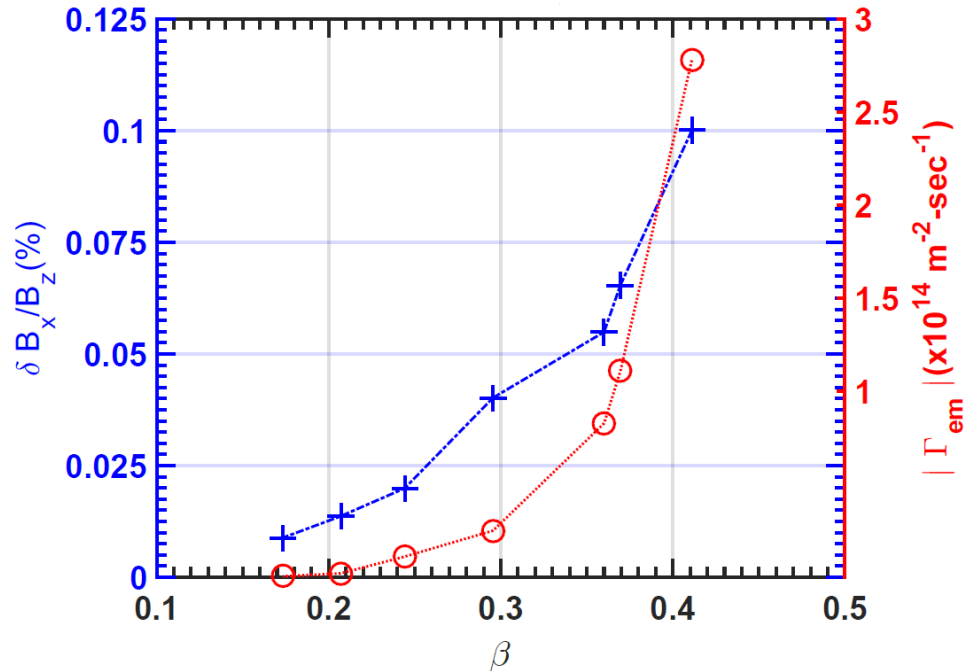
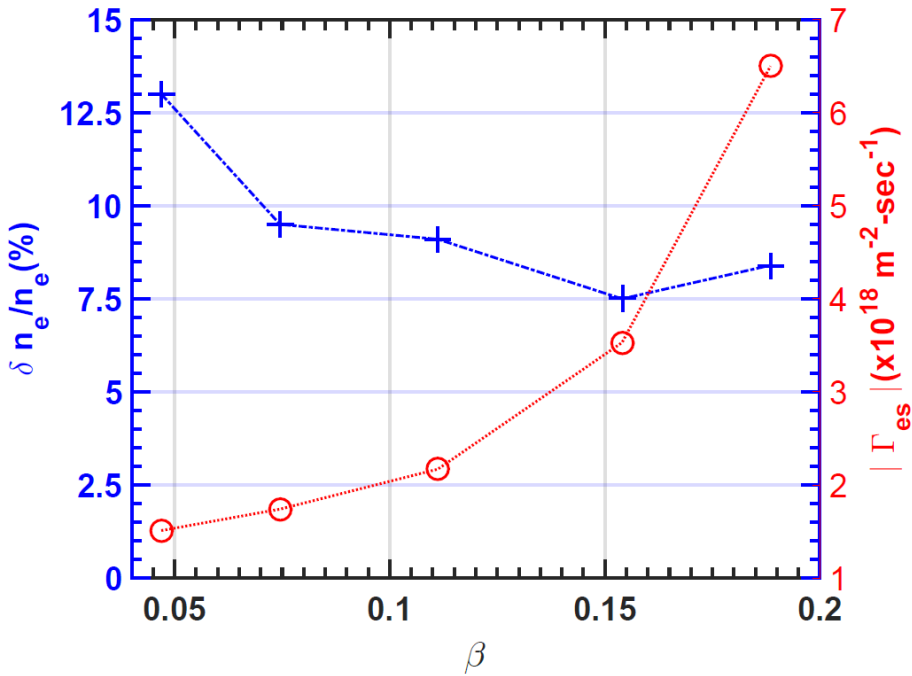


II. Study of electromagnetic particle flux



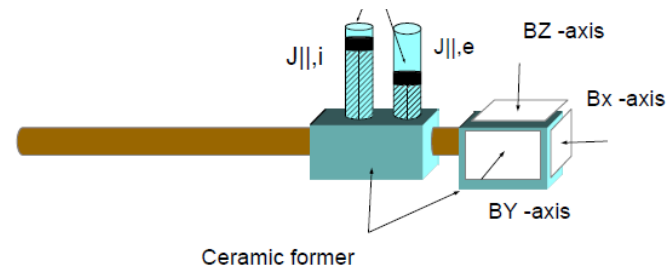
II. Study of electromagnetic particle flux

❑ Plasma beta, β effect on electrostatic and electromagnetic flux



$$\Gamma_{es} = \langle \delta n_e \delta v_r \rangle$$

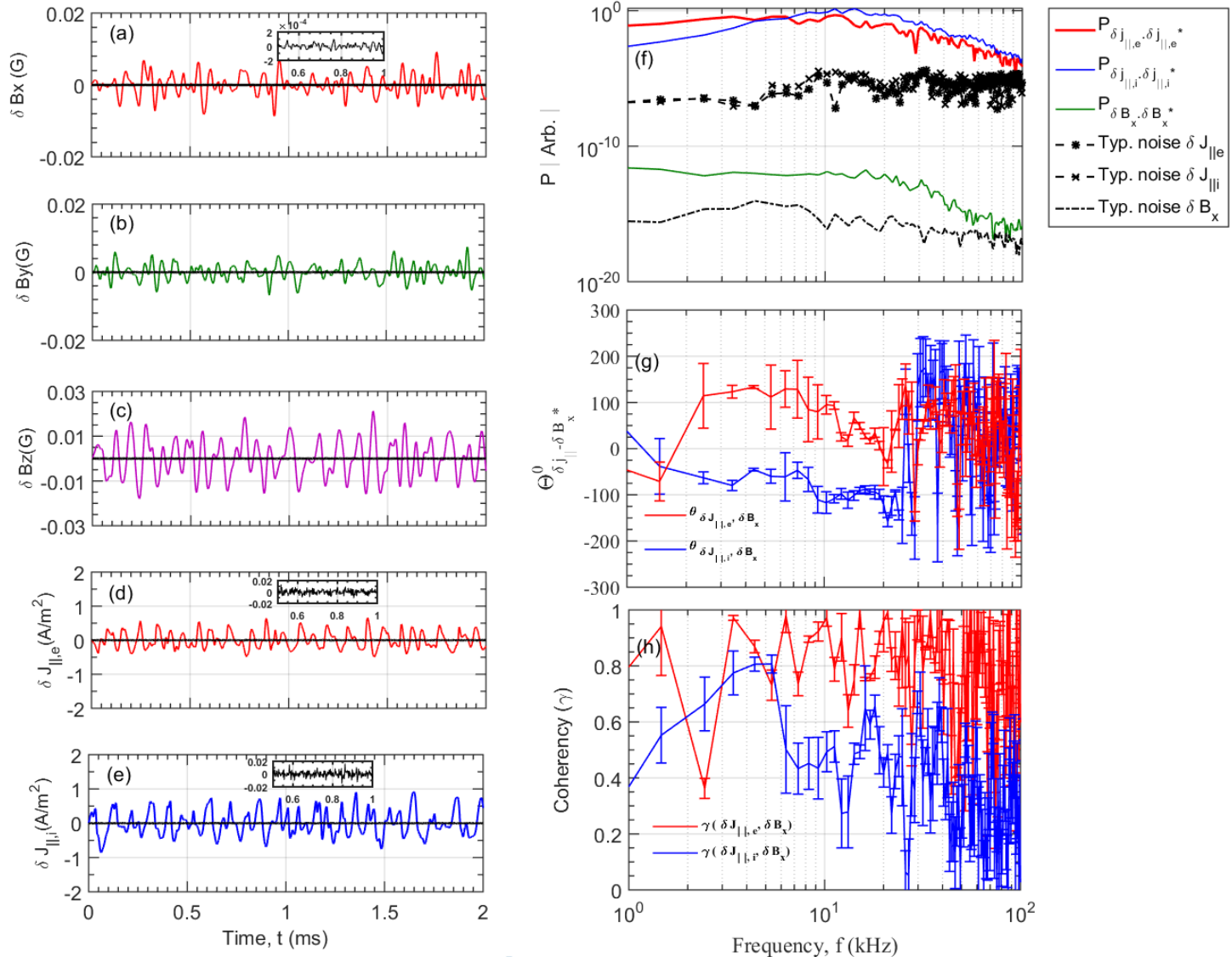
$$\Gamma_{em}^{i,e} = \frac{\langle \delta J_{\parallel,i,e} \delta B_r \rangle}{q_{i,e} B_z}$$





II. Study of electromagnetic particle flux

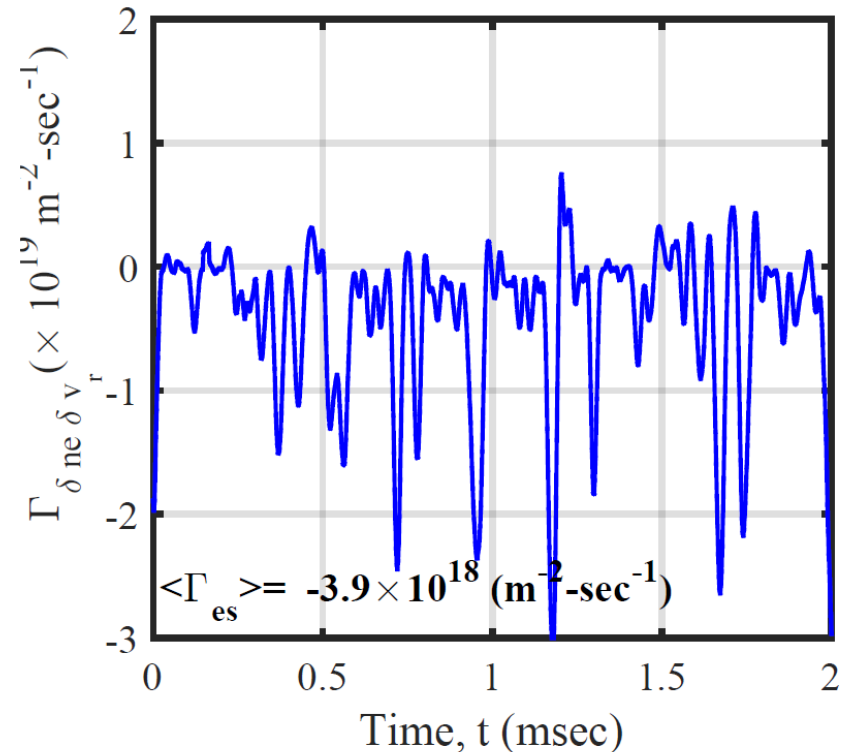
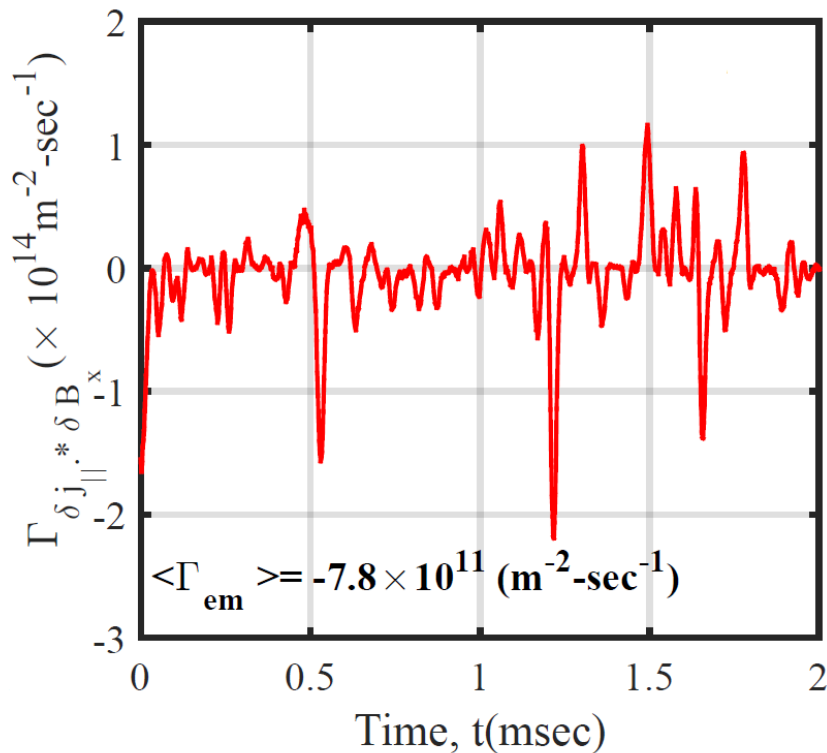
Temporal and Spectral Characteristics of Fluctuations





II. Study of electromagnetic particle flux

- A comparison of particle flux due to electrostatic and electromagnetic fluctuations



✓ The obtained ratio of EM to Electrostatic flux is, $\left| \frac{\Gamma_{em}}{\Gamma_{es}} \right| \approx 10^{-5} \text{ ?}$



II. Study of electromagnetic particle flux

Understanding of electromagnetic particle flux

Electromagnetic electron particle flux is given by,

$$\Gamma_{em} \approx \langle \delta J_{\parallel e} \delta B_r \rangle = \langle \delta J_{\parallel} \delta B_r \rangle = \langle \nabla_{\perp}^2 A_{\parallel} \frac{\partial}{\partial y} A_{\parallel} \rangle = \text{Real} \left(\sum_{\vec{k}} i k_{\perp}^2 k_y |A_{\parallel}|^2 \right) = 0$$

If the total parallel current is $\delta J_{\parallel} = \delta J_{\parallel e} + \delta J_{\parallel i}$. Then the electron flux will

$$\Gamma_{em}^e = \frac{1}{eB} \langle \delta J_{\parallel i} \delta B_x \rangle - \frac{1}{eB} \frac{c}{4\pi} \frac{\partial}{\partial x} \langle \delta B_x \delta B_y \rangle - \frac{1}{eB} \frac{c}{4\pi} \langle \delta B_y \frac{\partial}{\partial z} \delta B_z \rangle$$

$$\Gamma_{em}^e = \frac{1}{eB} \langle \delta J_{\parallel i} \delta B_x \rangle = -\frac{\beta_e m_e}{m_i} n_o c_e \sum_{\vec{k}} \frac{k_{\parallel} c_e k_y \rho_e}{|\omega|^2} \delta_k [\gamma \text{Im}(R_A) + \omega_r \text{Real}(R_A)] \left| \frac{e \delta \phi_k}{T_{eo}} \right|^2$$

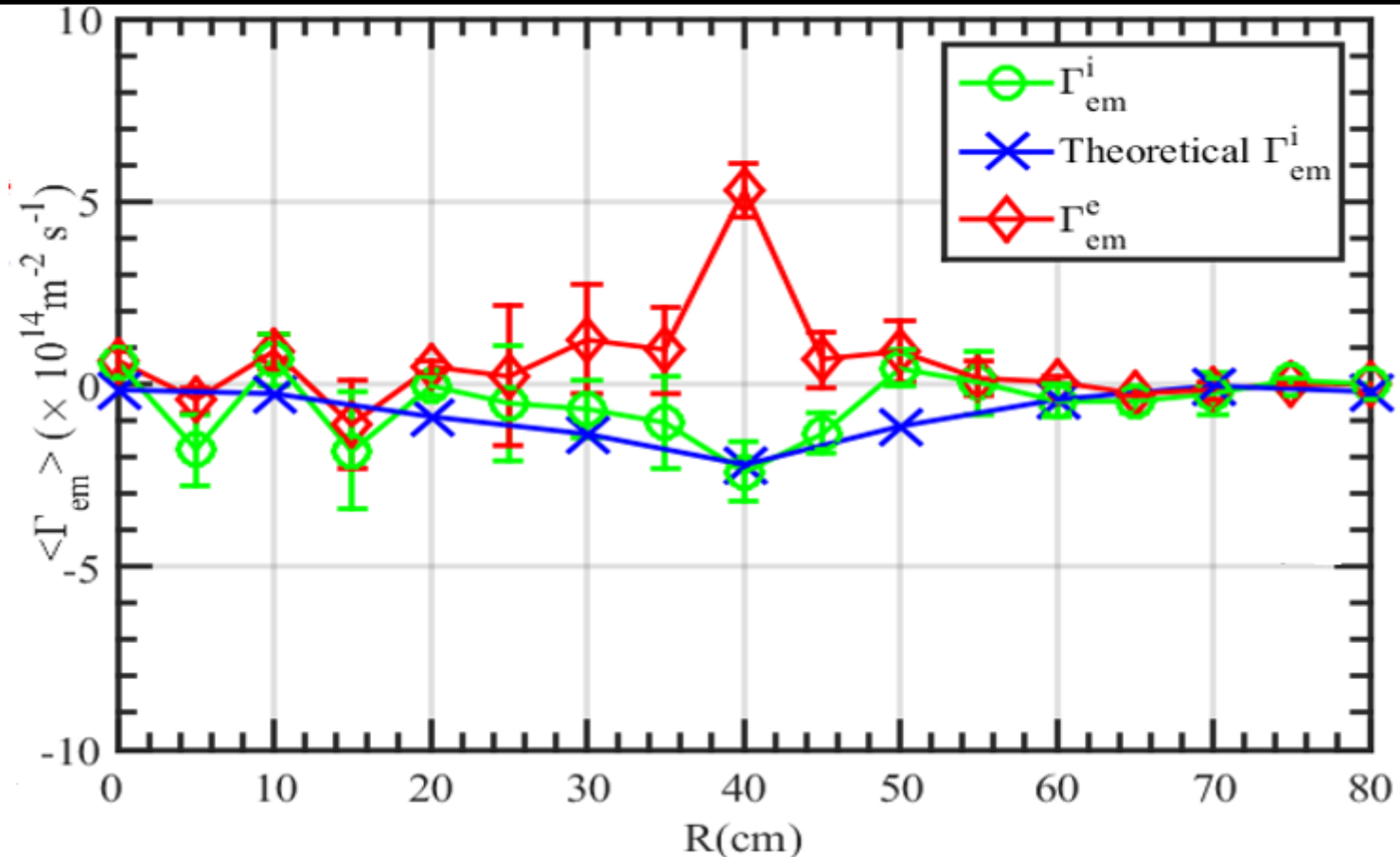
Hence, the ratio of electromagnetic to electrostatic particle flux is obtained as

$$\frac{\Gamma_{em}^e}{\Gamma_{es}^e} \approx \frac{\beta_e m_e}{2m_i \tau_e} \times (10 \sim 100) \approx 10^{-5}$$



II. Study of electromagnetic particle flux

$$\Gamma_{em}^i = -\frac{\beta_e m_e}{m_i} n_o c_e \sum_{\vec{k}} \frac{k_{\parallel} c_e k_y \rho_e}{|\omega|^2} \delta_k [\gamma \text{Im}(R_A) + \omega_r \text{Real}(R_A)] \left| \frac{e \delta \phi_k}{T_{eo}} \right|^2$$



$$\Gamma_{em}^e = \frac{1}{eB} \langle \delta J_{\parallel i} \delta B_x \rangle - \frac{1}{eB} \frac{c}{4\pi} \frac{\partial}{\partial x} \langle \delta B_x \delta B_y \rangle - \frac{1}{eB} \frac{c}{4\pi} \langle \delta B_y \frac{\partial}{\partial z} \delta B_z \rangle$$



III. Study of heat flux

- ❖ Study of total flux due to fluctuations in the background of ETG turbulence leads to the study of turbulent particle flux and heat flux simultaneously.
- ❖ Since particle flux is already characterised for ETG turbulence, hence we will be measuring the heat flux.

- ❖ Energy/heat flux is basically defined as

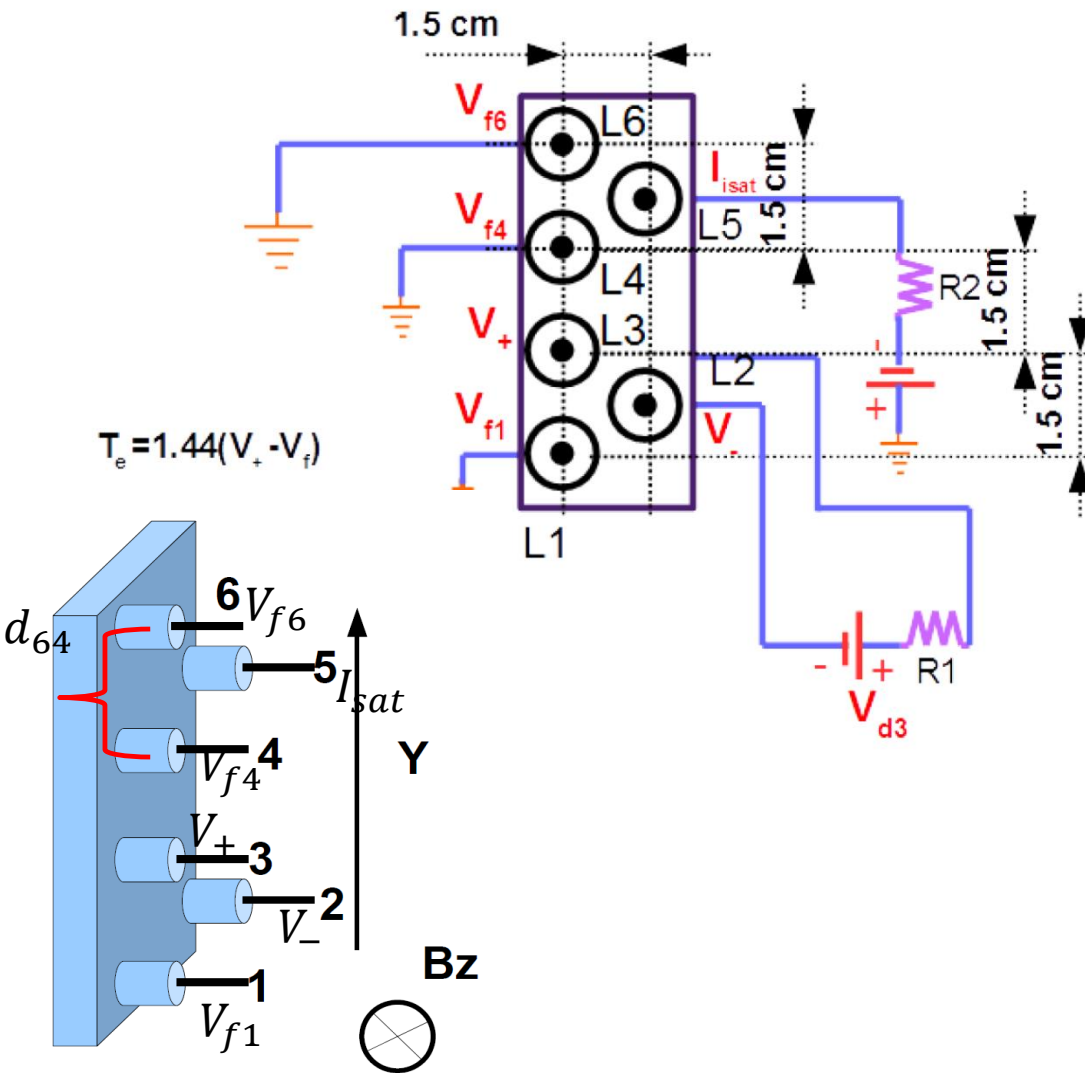
$$Q_e = \frac{3}{2} \langle \tilde{v}_r (n_o \tilde{T}_e + \tilde{n} T_e) \rangle = \frac{3}{2} n_o \langle \tilde{T}_e \tilde{v}_r \rangle + \frac{3}{2} T_e \langle \tilde{n} \tilde{v}_r \rangle$$

Conductive Heat flux (q) Convective Heat flux (q)

- ❖ Investigation Activity for Study of heat flux can be subdivided in following category:
 - ✓ Diagnostic Development for accurate measurement of real time temperature fluctuations and Heat flux
 - ✓ Validation for T_e and δT_e
 - ✓ Investigation of Heat flux in ETG background
 - ❑ Theoretical Estimation and its Comparison with experimental observations



III. Study of heat flux



$$\delta E_\theta = - \frac{(\delta \phi_{f6} - \delta \phi_{f4})}{d_{64}}$$

$$\delta T_e = \frac{V_+ - V_f}{\log(2)} \text{ where}$$

$$V_f = \frac{V_{f1} + V_{f4}}{2}$$

Particle flux

$$\Gamma = \langle \delta n_e \delta v_r \rangle$$

Conductive flux

$$q = \frac{3}{2} n_e \langle \delta T_e \delta V_r \rangle$$

where

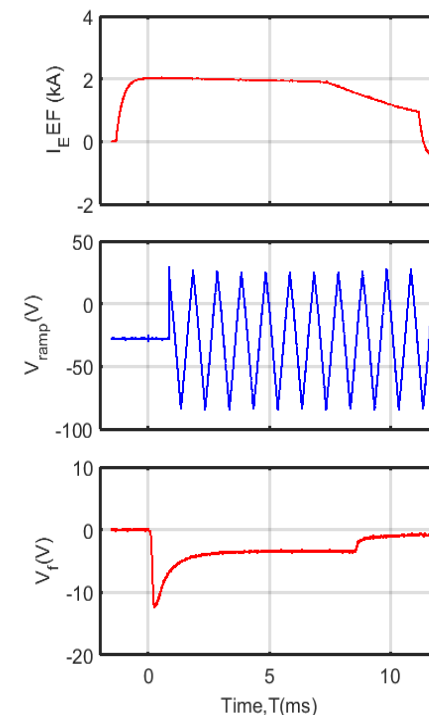
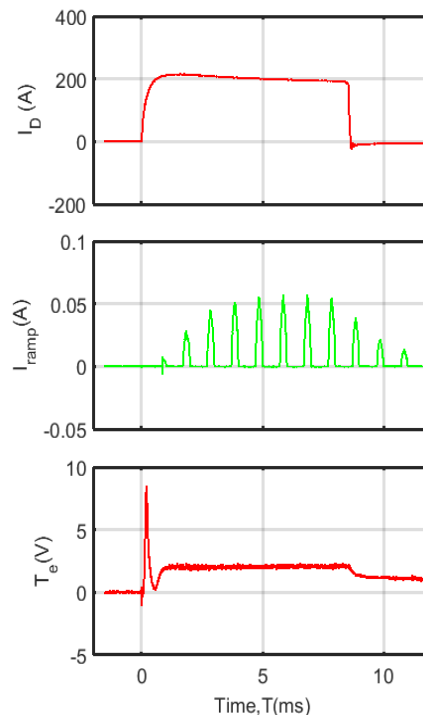
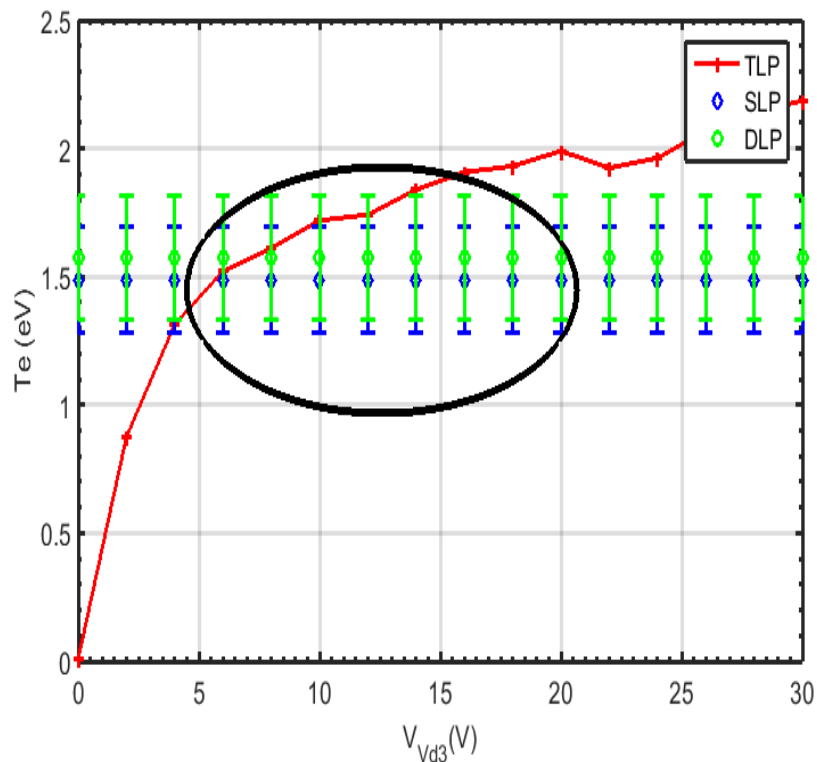
$$\delta V_r = \frac{\delta E_\theta \times \vec{B}_z}{B_z^2}$$

Schematic of Probe assembly for simultaneous measurement of particle flux, Γ_{es} and heat flux, q



III. Study of heat flux

❑ Selection of Bias voltage for T_e measurement with TLP

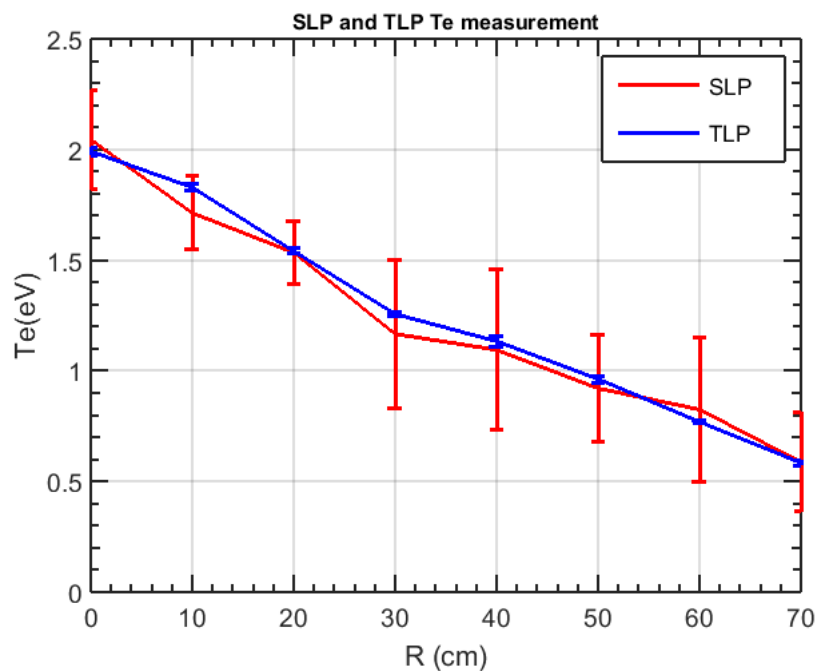


- ✓ For proper selection of fixed bias voltage V_{d3} we perform the T_e measurement for different V_{d3} and compared it with Single and Double probes measurement
- ✓ It is found that the T_e measured with TLP is very close SLP and DLP measurement for 6.0V to 15.0 V i.e. $5V_{d2} < V_{d3} > 10V_{d2}$ where $V_{d2} \approx T_e/1.44T$

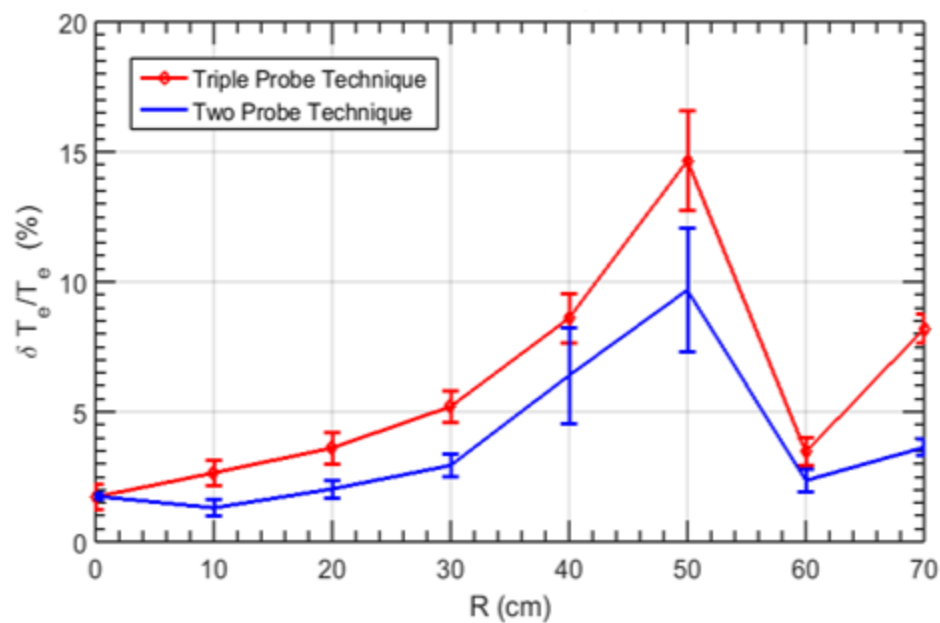


III. Study of heat flux

Comparison of mean T_e and fluctuations with other diagnostics



Radial Comparison of Mean T_e with SLP and TLP diagnostic

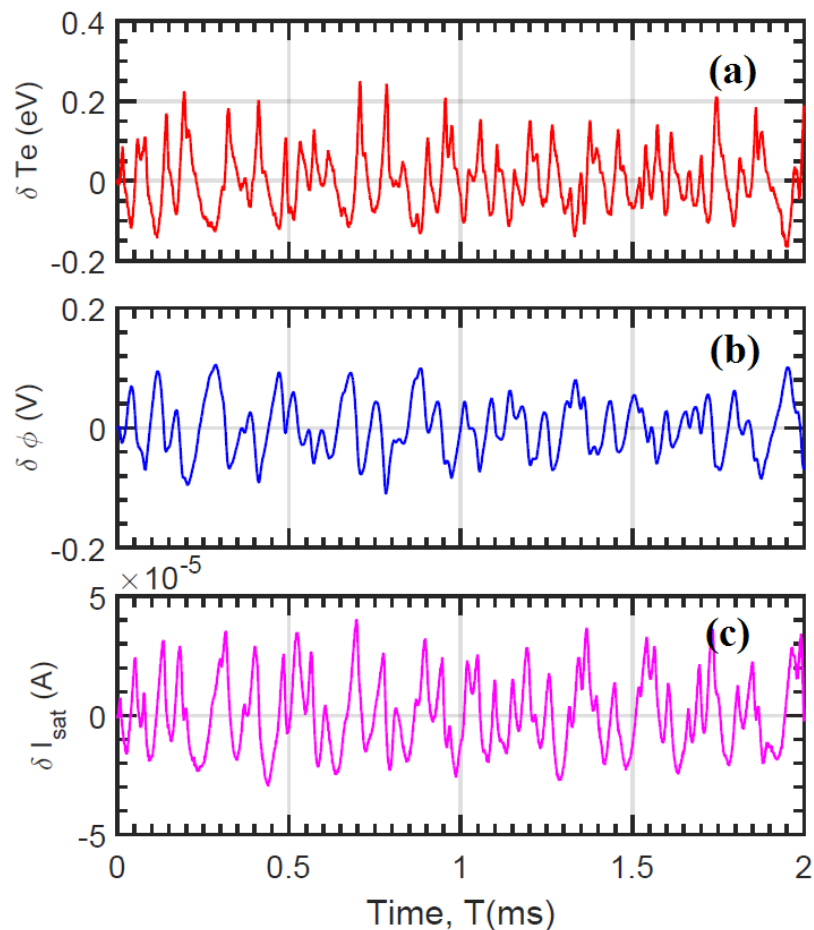


Temperature fluctuation comparison of TLP and Two probe diagnostic

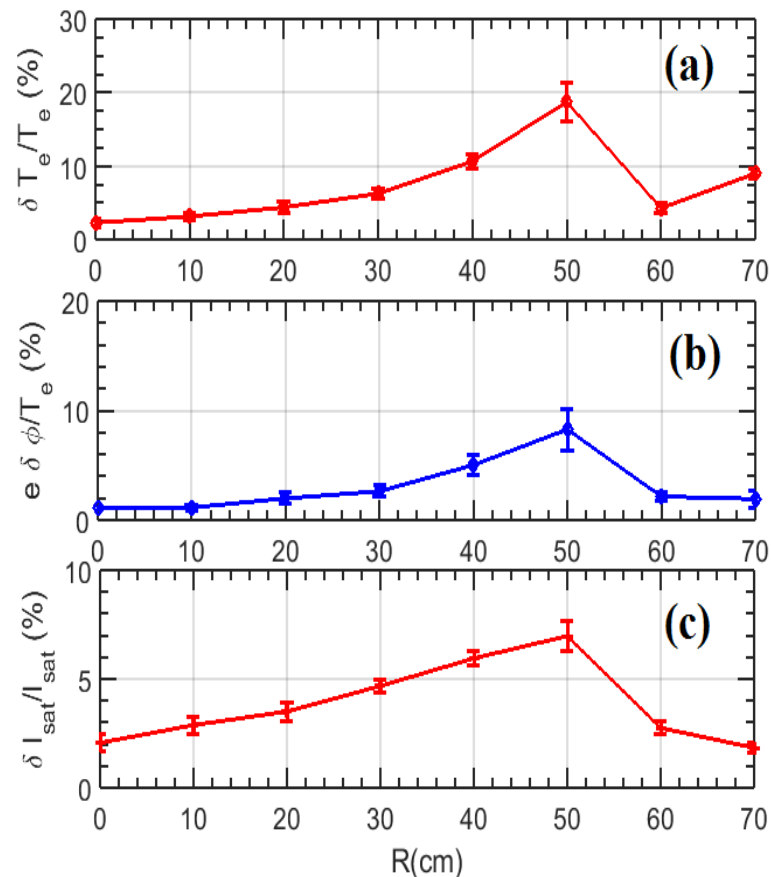


III. Study of heat flux

Fluctuation Measurement



Typical Fluctuations time profile for steady state at R=0 cm

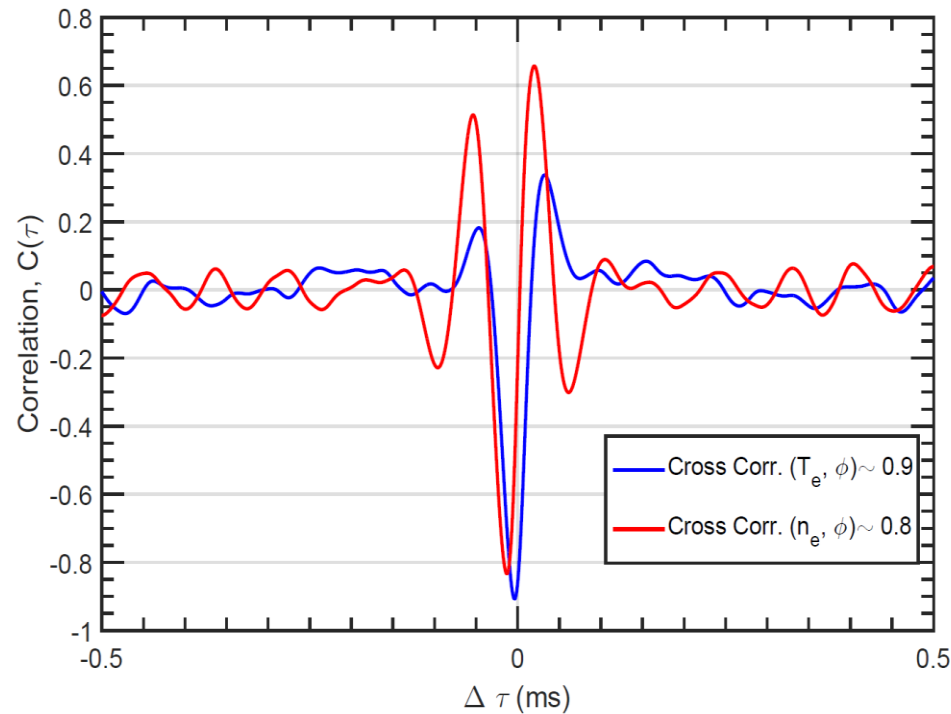


Radial profile of fluctuation observed

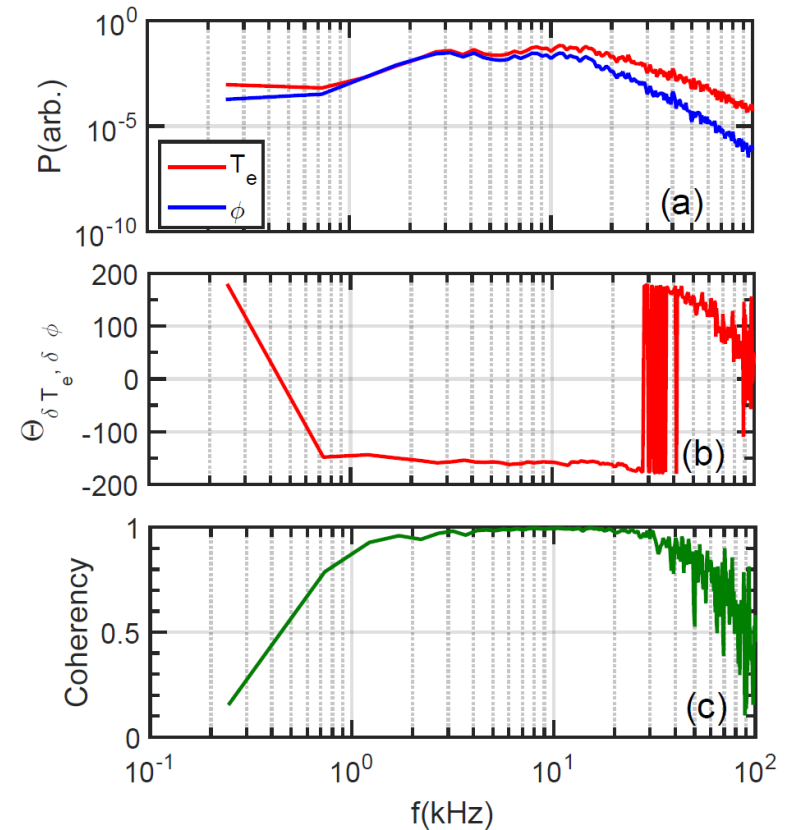


III. Study of heat flux

Fluctuation Characterization



Correlation Temperature and density fluctuations with potential fluctuations



Power spectra, phase angle and coherency plot of Temperature fluctuations and potential fluctuations



III. Study of heat flux

Phase angle comparison with ETG turbulence

- Further justification for temperature fluctuation is done with phase angle measurement with respect to potential fluctuations

Basic Equations for W-ETG is as follows;

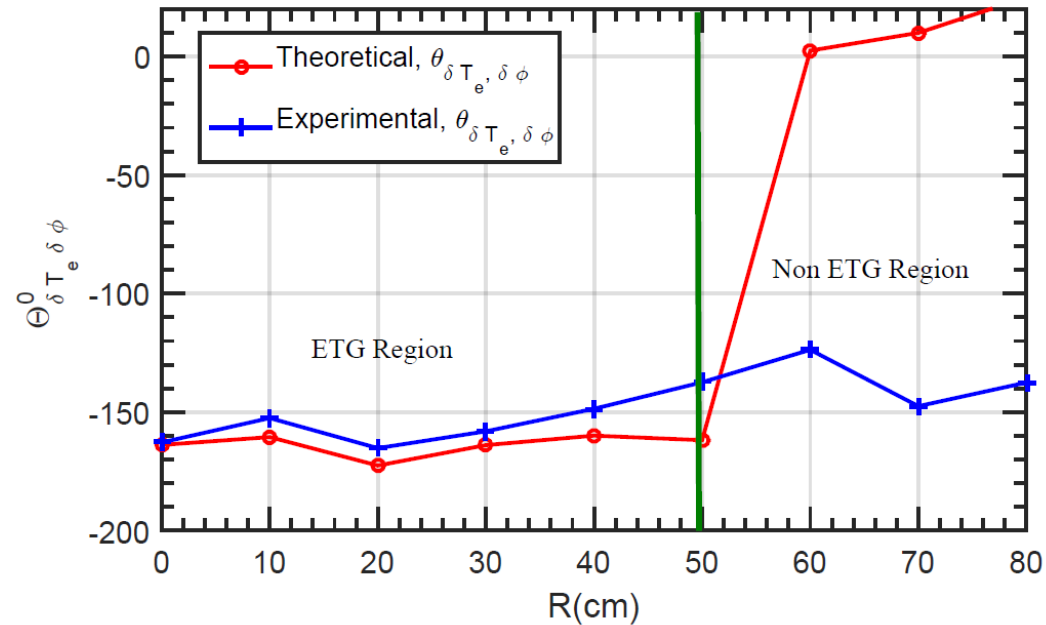
$$\tilde{n} = -\tau^* \tilde{\phi}$$

$$\tilde{T}_e = \left[\left(\frac{1}{L_{T_e}} - \frac{2}{3} \frac{1}{L_n} \right) \frac{k_y \rho_e c_e}{\omega} - \frac{2}{3} \tau^* \right] \tilde{\phi}$$

Where

$$\tau^* = \frac{T_e}{T_i} \left[1 + i\sqrt{\pi} \frac{\omega}{k_{\perp} v_{thi}} \exp\left(-\frac{\omega^2}{k_{\perp}^2 v_{thi}^2}\right) \right]$$

By considering ion non-adiabatic response.

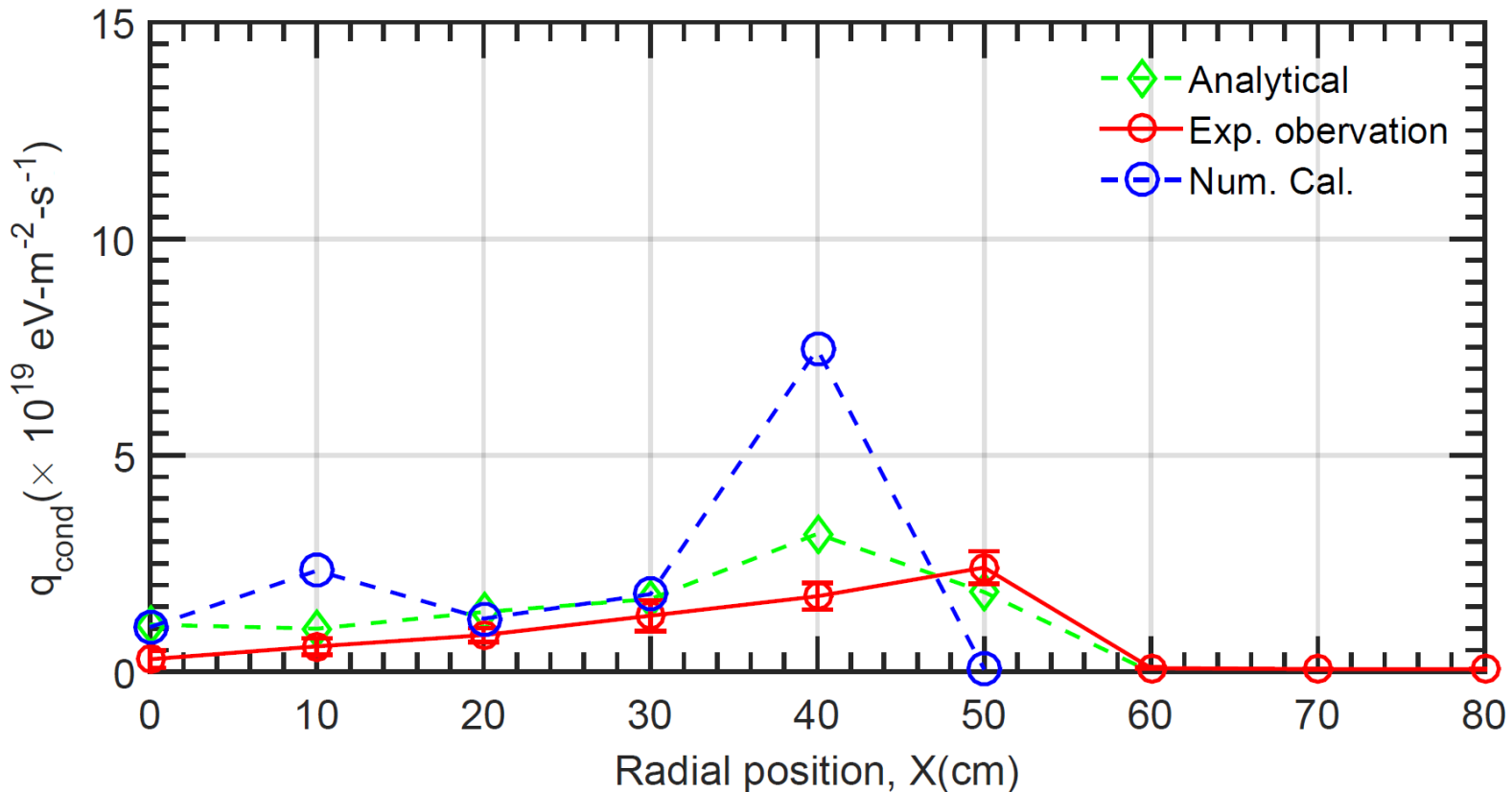


Phase Angle comparison between temperature fluctuation and potential fluctuations



III. Study of heat flux

Conductive heat flux and its comparison



$$q = \frac{3}{2} n_o \langle \delta T_e \delta V_r \rangle = -\frac{3}{2} \sum_k \frac{k_y}{B} n_o |\tilde{T}_{e,k}| |\tilde{\phi}_k| \sin \theta_{T_e \phi} \quad \text{where } \theta_{T_e \phi} = \theta_{T_e} - \theta_{\phi}$$

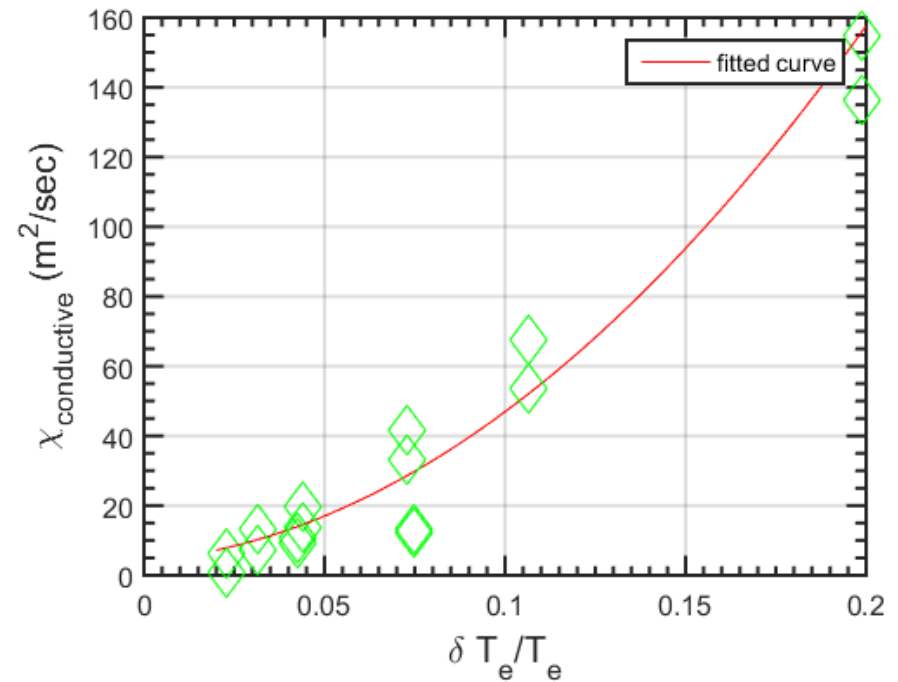
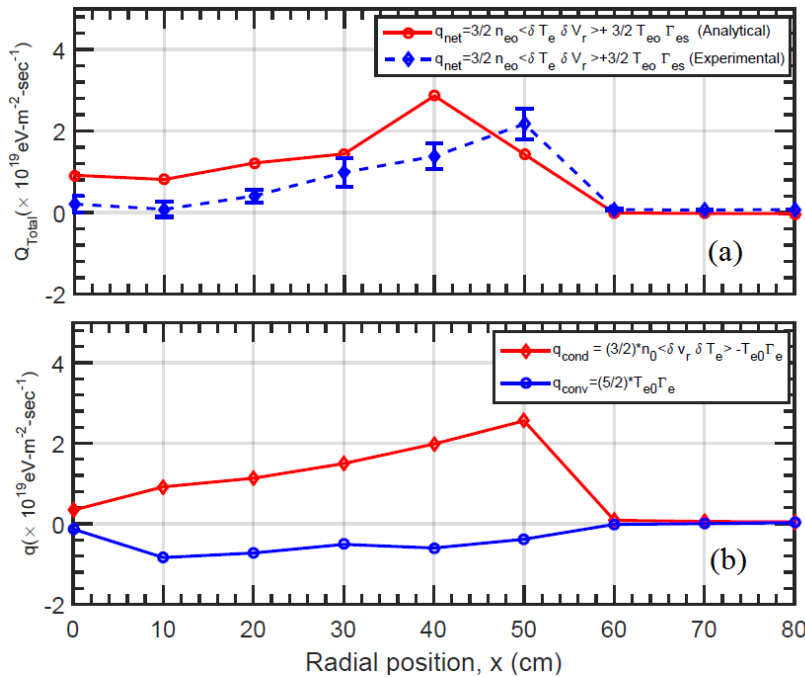
$$q_e = \frac{3}{2} n_o c_e T_{eo} \sum_k \left(\eta_e - \frac{2}{3} \right) \frac{c_e \gamma_k (k_y \rho_e)^2}{L_n |\omega|^2} \left| \frac{e \delta \phi_k}{T_{eo}} \right|^2 + T_{eo} \Gamma_e$$



III. Study of heat flux

- (a) Radial variation of total heat fluxes and
- (b) Comparison of convective heat fluxes.

Electron thermal conductivity due to temperature fluctuations present in the system.



❖ Observation shows that thermal conductivity exhibits a quadratic dependency for the normalized fluctuations for levels between 5% and 20%.



Summary & Conclusion

1. Inward particle transport due to electrostatic fluctuations is observed

(*Srivastav et al., Physics of Plasmas 24, 112115 (2017)*)

- i. Net particle flux results from the phase difference between the density and potential fluctuations, other than 180 degrees for ETG driven modes.
- ii. The experimental cross phase angle and flux have been compared with the cross phase and flux resulting due to the non-adiabatic ion response due to the resonant interaction of the ions with the ETG mode $k_{\perp} V_{thi} \sim \omega$.
- iii. The experiment and theoretical results quantitatively follow the same trend across the radius and match within 20% with each other.



Summary & Conclusion

2. Particle transport due to electromagnetic fluctuations is experimentally estimated observed and theoretical model is proposed

(Srivastav et al., Plasma Phys. Control. Fusion 61, 055010 (2019))

- i. Theory for particle flux due to electromagnetic fluctuation is developed and we found the ratio of electromagnetic flux to electrostatic flux is in agreement with our experimental findings in ETG background .
- ii. Experimentally obtained ion flux values agrees well with numerically obtained values using theoretical model of electromagnetic flux.
- iii. Non-ambipolar EM flux is observed at $R=40$ cm which may be one cause of change in potential profile at $R=40$ cm that leads us to create a shear flow in poloidal direction.



Summary & Conclusion

3. Heat transport due to electrostatic fluctuations is measured and compared with theoretical model

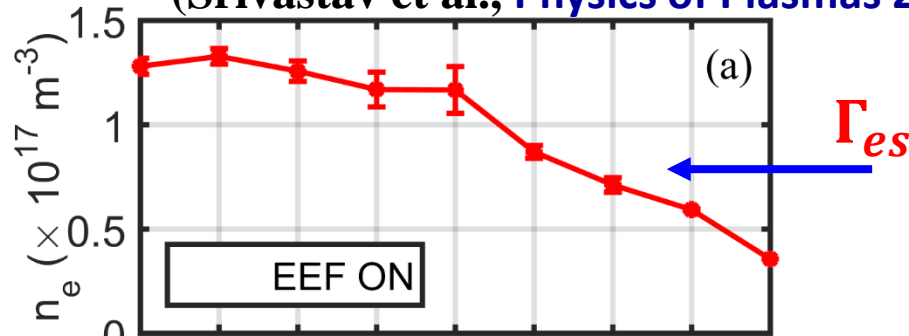
(Srivastav et al., Physics of Plasmas 26, 052303 (2019))

- i. Mean temperature measurements using TLP are validated with SLP and temperature fluctuation is validated by two probe technique before applying for real time temperature fluctuations.
- ii. Radial measurement of phase angle is supported by theoretical model of ETG turbulence for $R \leq 50 \text{ cm}$.
- iii. Radial measurement of heat flux is obtained by simultaneous measurement of fluctuations in T_e and ϕ_f which is in good agreement with theoretical estimations.

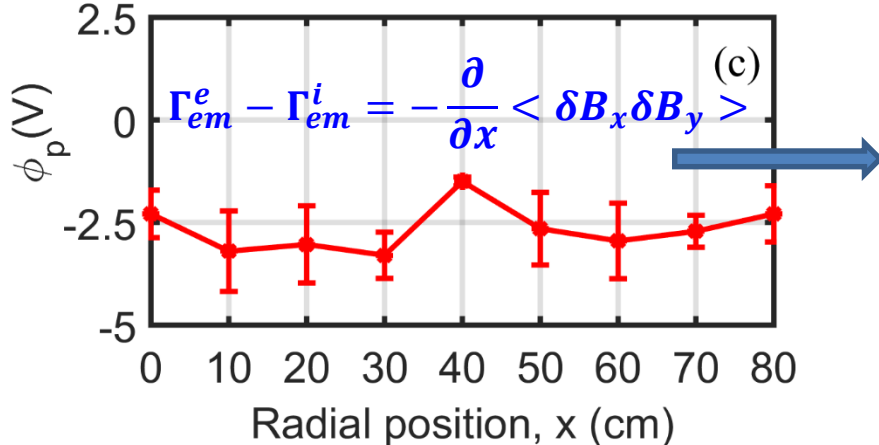
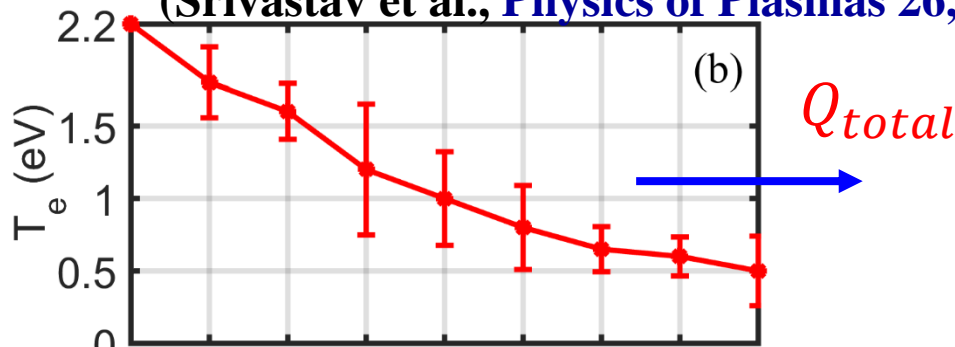


Summary & conclusion

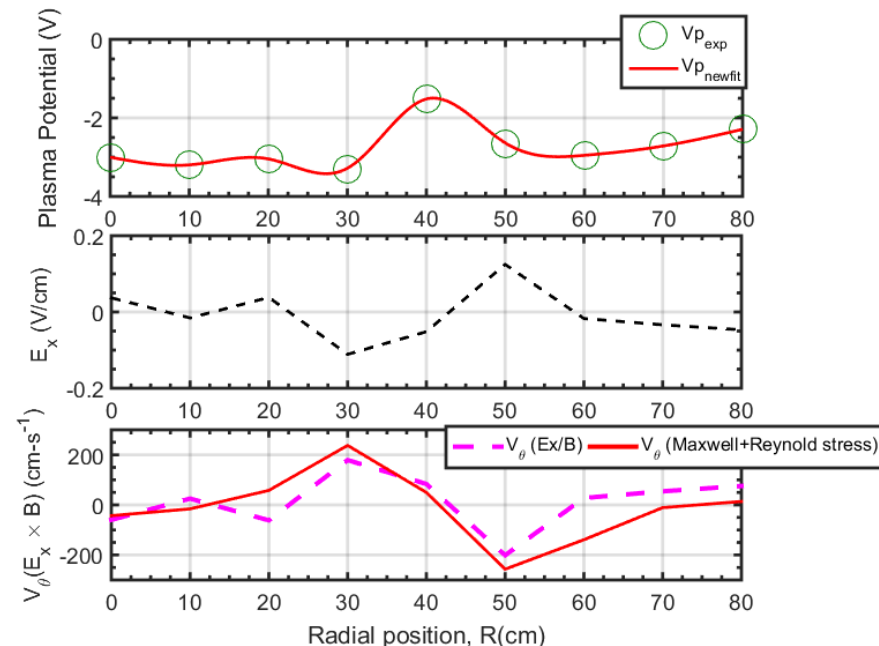
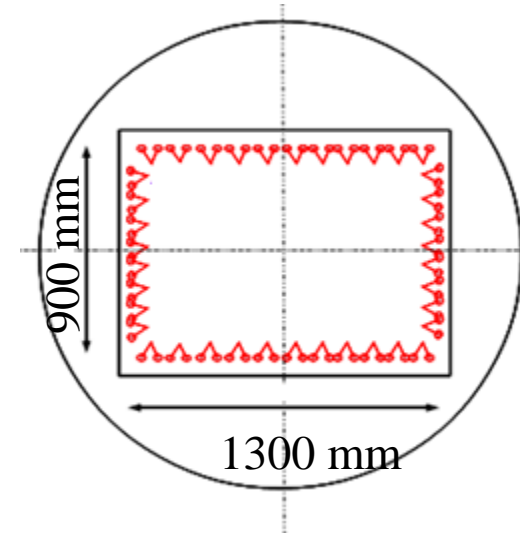
(Srivastav et al., *Physics of Plasmas* 24, 112115 (2017))



(Srivastav et al., *Physics of Plasmas* 26, 052303 (2019))



(Srivastav et al., *Plasma Phys. Control. Fusion* 61, 055010 (2019))





Acknowledgement



Late Prof. P.K. Kaw

Collaborators



Dr. Lalit Mohan Awasthi
Scientific Officer –
G, Head of LVPD



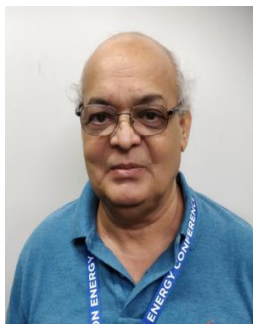
Dr. Amulya Kumar Sanyasi
Scientific Officer - D



Mr. Pankaj Kumar Srivastava
Scientific Officer - D



Dr. Ritesh Sugandhi
Scientific Officer - F



Prof. Raghvendra Singh
Senior Professor (Retired)
Senior Researcher, NFRI,
Republic of Korea



Dr. Rameshwar Singh
Postdoctoral Researcher –
University of California San
Diego

Thank you for your kind attention



Diffusion of electrons across magnetic field of EEF

Cold Electrons :

$$T_e \sim 1.0 \text{ eV}, \quad n_e \sim 3 \times 10^{11} \text{ cm}^{-3}, \quad B = 160 \text{ Gauss}$$

$$\nu_{ei} = n_i \sigma v_e = 1.3 \times 10^7 \text{ s}^{-1}, \quad \lambda_f^c \sim 3 \text{ cm}$$

Avg. dis. $\sim 600 \text{ cm}$, suffers 200 collisions

$$\rho_{ec} \sim 0.015 \text{ cm}, \quad \text{Perp. dis. by cold electron} \sim 3 \text{ cm}$$

Hot Electrons

$$T_e \sim 23 \text{ eV} \quad \nu_{en} = n_n \sigma v_e = 1.0 \times 10^6 \text{ s}^{-1}, \quad \lambda_f^h = 200 \text{ cm}$$

Avg. dis. $\sim 600 \text{ cm}$, suffers 3 collisions

$$\rho_{eh} \sim 0.08 \text{ cm} \quad \text{Perp. dis. by hot electron} \sim 0.24 \text{ cm}$$

- Since majority of the experimental studies shows that the floating potential fluctuation measurement with conventional Langmuir probe can be approximated with plasma potential fluctuation measurement as

$$\varphi_{pl} = \varphi_{fl} + \mu \frac{T_e}{e}$$

For fluctuation

$$\tilde{\varphi}_{pl} = \tilde{\varphi}_{fl} + \mu \frac{\tilde{T}_e}{e}$$

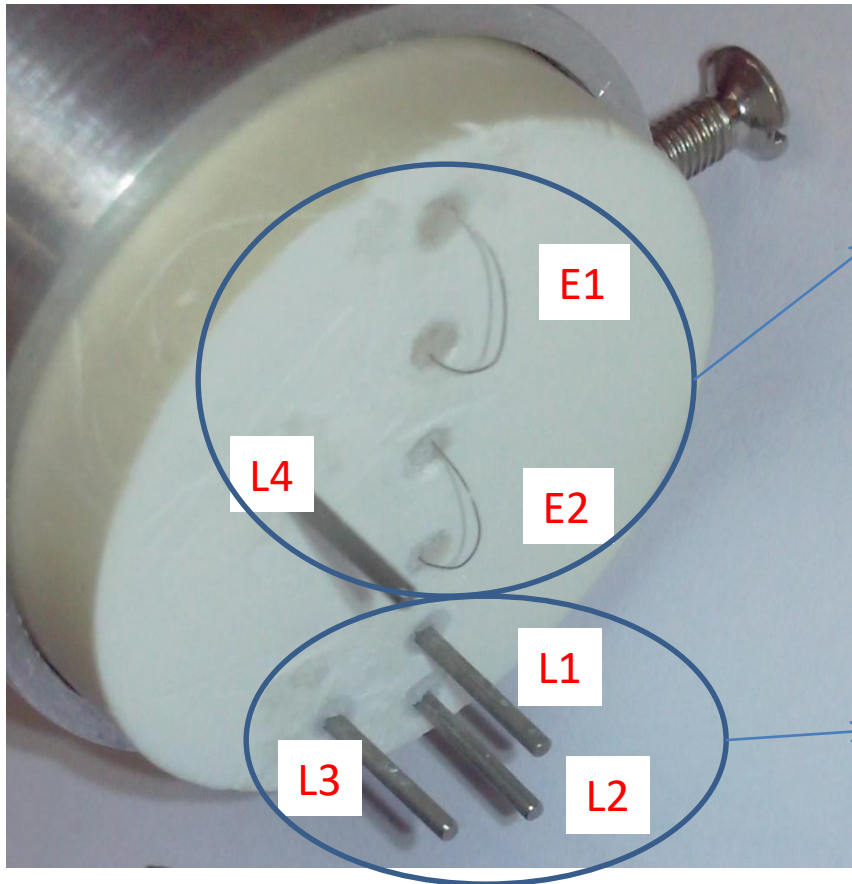
In absence of temperature fluctuations

$$\tilde{\varphi}_{pl} = \tilde{\varphi}_{fl}$$

So, poloidal electric field fluctuation can be calculated with floating potential fluctuations.

Hence, in presence of temperature fluctuation, above relation can't be considered as accurate

❑ New Probe assembly for Γ_{es} measurement, for ϕ_f and ϕ_p fluctuation measurement



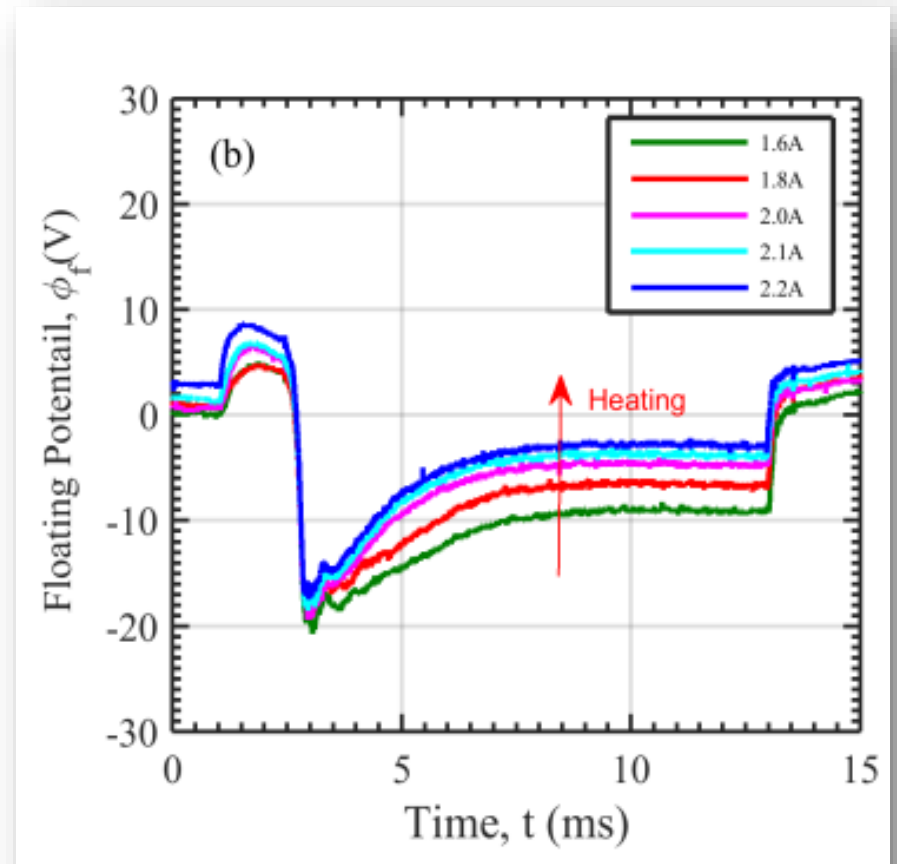
➤ Emissive Probe assembly to measure particle flux with plasma potential fluctuation along with ion-saturation fluctuation with conventional Langmuir probe [Diameter =0.2 mm, Length=10mm]

➤ Triple Probe assembly to measure particle flux with floating potential fluctuation measurement [Diameter =0.5mm, Length=10mm]

Validation of Plasma Potential measurement: Varying Heating current

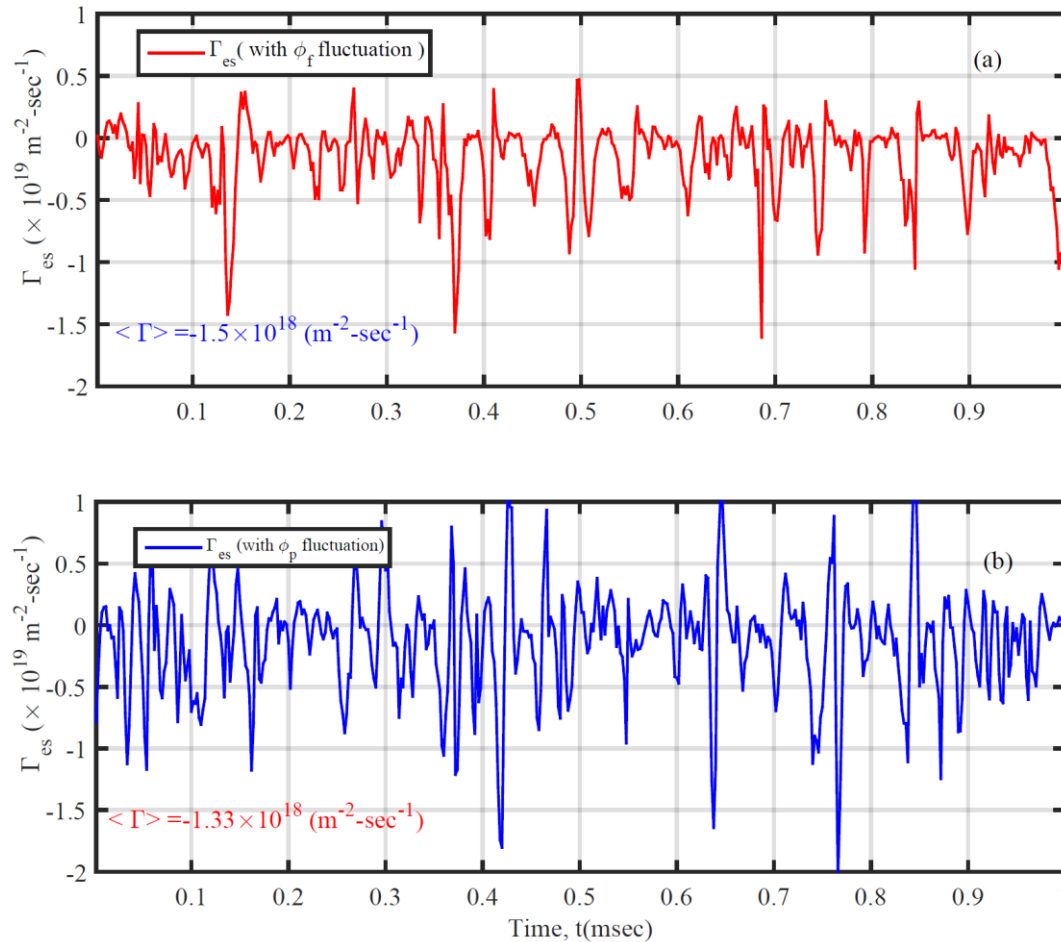
- ❑ The floating potential measurement with ≥ 2.0 Amp heating current shows no significant change.
- ❑ Implies heated filament works as emissive probe as it floats now at plasma potential.

✓ At $I_{\text{emissive}} \approx 2.1$ Amp, we measured plasma potential fluctuation for particle flux estimation.



Simultaneous measurement of floating potential with two emissive probe with different heating current

Comparison Plot for Electrostatic particle flux estimated with floating potential fluctuation ($\delta\phi_f$) and plasma potential fluctuation ($\delta\phi_p$)



- ❖ No significant deviation is observed in particle flux measurement with ϕ_p and ϕ_f fluctuation measurement.
- ❖ This is only possible when Temperature fluctuations are completely cancels out in poloidal electric field fluctuation calculations.

Particle flux measured with floating potential fluctuation and plasma potential fluctuation for comparison.